General Disclaimer

One or more of the Following Statements may affect this Document

- This document has been reproduced from the best copy furnished by the organizational source. It is being released in the interest of making available as much information as possible.

- This document may contain data, which exceeds the sheet parameters. It was furnished in this condition by the organizational source and is the best copy available.

- This document may contain tone-on-tone or color graphs, charts and/or pictures, which have been reproduced in black and white.

- This document is paginated as submitted by the original source.

- Portions of this document are not fully legible due to the historical nature of some of the material. However, it is the best reproduction available from the original submission.

Produced by the NASA Center for Aerospace Information (CASI)

TRW Space &
Technology Group

TRW

Report No.
CR-167953

Deep Discharge Reconditioning and Shorted Storage of Batteries

Final Report

(NASA-CR-167953) DEEP DISCHARGE RECONDITIONING AND SHORTED STORAGE OF BATTERIES Final Report (TRW, Inc., Redondo Beach, Calif.) 72 p HC A04/MF A01 CSCL 10C G3/44

N83-10502

Unclas
35510

Prepared by
P. F. Ritterman

Prepared for
National Aeronautics and Space Administration
Lewis Research Center
21000 Brookpark Road
Cleveland, OH. 44135

Contract No.
321253

1. Report No.	2. Goverment Accession No.	3. Recipient's Catalog No.
CR-167953		

4. Title and Subtitle	5. Report Date
DEEP DISCHARGE RECONDITIONING AND SHORTED STORAGE BATTERIES	May 1982
	6. Performing Organization Code
7. Author	8. Performing Organization Report No.
Paul F. Ritterman	
9. Performing Organization Name and Address	10. Work Unit No.
TRW Redondo Beach, California 90278	11. Contract or Grant No. NAS 321253
	13. Type of Report and Period Covered
12. Sponsoring Agency Name and Address	
National Aeronautics and Space Administration 21000 Brookpark Road Cleveland, Ohio 44135	14. Sponsoring Agency Code

15. Supplementary Notes

Final Report

Project Manager, Dan Soltis - Solar and Electrochemistry Division

NASA Lewis Research Center, Cleveland, Ohio 44135

16. Abstract

The identification and measurement of hydrogen recombination in sealed nickel-cadium cells has made deep reconditioning on a battery basis safe and feasible. Deep reconditioning has been shown to improve performance and increase life of nickel-cadium batteries in geosynchronous orbit applications. The hydrogen mechanism and supporting data are presented. Parameter cell design experiments are described which have lead to the definition of nickel-cadium cells capable of high rate overdischarge without detriment to specific energy. Nickel-cadium calls of identical optimum design were successfully cycled for 7 seasons in simulation of geosynchronous orbit at 75 percent depth-of-discharge with extensive midseason and end-of-season overdischarge at rates varying from C/20 to C/4. Destructive physical analysis and cycling data indicated no deterioration or the development of dangerous pressures as a result of the cycling with overdischarge.

17. Key Words (Suggested by Author)	18. Distribution Statement
Nickel-Cadium Hydrogen Recombition Overdischarge	Unclassified - unlimited

19. Security Classif. (of this report)	20. Security Classif. (of this page)	21. No. of Pages	22. Price
Unclassified	Unclassified	63	

TRW Space &
Technology Group

TRW

Report No.
CR-167953

Deep Discharge Reconditioning and Shorted Storage of Batteries

Final Report

Prepared by
P. F. Ritterman

Prepared for
National Aeronautics and Space Administration
Lewis Research Center
21000 Brookpark Road
Cleveland, OH. 44135

Contract No.
321253

CONTENTS

CONTENTS (Continued)

FIGURES

FIGURES (Continued)

TABLES

TABLES (Continued)

TABLES (Continued)

ABSTRACT

The identification and measurement of hydrogen recombination in sealed nickel-cadmium cells has made deep reconditioning on a battery basis safe and feasible. Deep reconditioning has been shown to improve performance and increase life of nickel-cadmium batteries in geosynchronous orbit applications. The hydrogen mechanism and supporting data are presented. Parameter cell design experiments are described which have lead to the definition of nickel-cadmium cells capable of high rate overdischarge without detriment to specific energy. Nickel-cadmium cells of identical optimum design were successfully cycled for 7 seasons in simulation of geosynchronous orbit at 75 percent depth-of-discharge with extensive mid- and end-of-season overdischarge at rates varying from C/20 to C/4. Destructive physical analysis and cycling data indicated no deterioration or the development of dangerous pressures as a result of the cycling with overdischarge.

1. INTRODUCTION

The voltage, performance, and cycle life of sealed-cell, nickel-cadmium (Ni-Cd) batteries in geosynchronous orbit can be improved significantly by periodic deep reconditioning to a battery voltage of less than 1.0 volt. This has been demonstrated by TRW in both accelerated and real time laboratory simulation. It has also been shown that deep discharge reconditioning is not harmful to any of the battery cells despite the fact that some cells are pushed into overdischarge when deep reconditioning (accomplished by placing a resistor across the entire battery) is performed. Overdischarge had been thought to result in excessive and even dangerous cell pressures.

A study was made at TRW prior to the initiation of this contract, to determine and attempt to explain the behavior of Ni-Cd cells during overdischarge at rates usually encountered during battery deep discharge reconditioning. Both new and extensively cycled state-of-the-art Ni-Cd cells equipped with pressure-sensing devices were individually subjected to constant current overdischarge at C/200 to C/12 rates. In every case, hydrogen was the only gas evolved, and the rate of pressure rise was considerably less than theoretically expected from the overdischarge current. At the C/100 overdischarge rate and below, all cells tested reached pressure equilibrium and could apparently be overdischarged indefinitely at constant pressure and without exhaustion of negative electrode capacity as manifested by cell voltage remaining at -0.2 volt well beyond the set negative precharge capacity.

As part of the early study, it was also demonstrated that completely discharged Ni-Cd cells consumed hydrogen on open circuit stand at a rate directly proportional to hydrogen pressure.

The experiments mentioned above and other corroborating experiments lead to the postulation of the hydrogen recombination theory as an explanation of observed Ni-Cd cell behavior during low-rate overdischarge. The theory, presented in greater detail later in the report, states that hydrogen generated at the positive electrode during overdischarge reacts with cadmium hydroxide, the active material of the negative in the discharged state, to form cadmium and water. Thus, as the overdischarge proceeds,

hydrogen is generated and consumed while the negative electrode is discharged electrochemically and charged chemically. At a certain pressure, the rate of overdischarge and recombination balance and equilibrium is achieved.

The ability of state-of-the-art Ni-Cd cells to sustain continuous low-rate overdischarge, via hydrogen recombination, suggested that, with the optimization of certain cell parameters, the rate of hydrogen recombination and, hence, safe overdischarge rate could be significantly increased. By developing battery cells with increased overdischarge rate capabilities, greater flexibility in reconditioning rate choices would result as well as the reduction of the complexity of battery bypass circuitry. A battery made with such cells would have a lower weight, lower cost, and higher reliability allowing for growth in payload size and spacecraft life.

Development of Ni-Cd cells with high-rate overdischarge capability without adverse effect to normal performance was the goal of the NASA-funded study discussed in this report.

The objectives of this study were to: (1) verify and expand the scope of the hydrogen recombination mechanism for sealed Ni-Cd cells; (2) define a Ni-Cd cell design which has optimum hydrogen recombination and, hence, overdischarge rate capability; (3) based on the results of (2), design, build, and evaluate cells capable of sustaining high-rate overdischarge, without sacrificing life, specific energy, and performance; and, (4) develop improved Ni-Cd cell electrodes with respect to performance, specific energy, and life when evaluated under cell design conditions which are optimum for hydrogen recombination.

Cells with significantly improved hydrogen recombination would result in Ni-Cd batteries which could not only be reconditioned more rapidly but also in batteries which would not require expensive and heavy electronic bypass equipment.

2. HYDROGEN RECOMBINATION MECHANISM

The half-cell reactions of a Ni-Cd cell during discharge are:

a) At the positive electrode:

$$2\beta NiOOH + 2H_2O + 2e \rightarrow 2\ Ni(OH)_2 + 2\ OH^- \quad (1)$$

b) At the negative electrode:

$$Cd + 2\ OH^- \rightarrow Cd(OH)_2 + 2e^- \quad (2)$$

Ni-Cd cells are designed to be positive limiting so that, when the positive electrode capacity exhausts, some cadmium (usually 30 percent of positive capacity) which can still be discharged remains. When discharge is continued beyond the exhaustion of positive capacity (as would be the case when a battery is shorted through a resistor and imbalance in cell capacity exists), the half-cell reactions are:

a) At the positive electrode:

$$2H_2O + 2e^- \overset{i_1}{\rightarrow} 2\ OH^- + H_2 \quad (3)$$

b) At the negative electrode:

$$Cd + 2\ OH^- \overset{i_1}{\rightarrow} Cd(OH)_2 + 2e^- \quad (2)$$

At low discharge rates, it can be assumed that, when cell voltage drops from 1.2 volts to about -0.05 volt, all of the current is used for reaction (3); the evolution of hydrogen: the discharge current equals i_1, which is the rate of hydrogen generation as well as cadmium oxidation expressed as a current.

The rate of hydrogen generation expressed as pressure rise per unit time is given by:

$$\frac{\Delta P}{\Delta t} = \frac{i_1\ RT^\circ}{2VF} \quad (4)$$

where R and F are the gas and Faraday's constants, T° is absolute temperature, and V is cell gas volume.

Hydrogen recombination is believed to occur during overdischarge of Ni-Cd cells because the rate of pressure rise is lower than predicted by

equation (4) and, in the case of low overdischarge rates, the net rate of pressure rise is zero.

Hydrogen recombination most likely occurs on the sintered nickel sites of the negative electrode where it is catalytically absorbed via

$$H_2 + Ni(sinter) \rightarrow 2H(Ni\ sinter) \quad (5)$$

The adsorbed hydrogen reacts with cadmium hydroxide which is in intimate contact with the sintered nickel sites on the negative electrode:

$$2H(Ni) + Cd(OH)_2 \rightarrow Cd + 2H_2O \quad (6)$$

Hydrogen may also be adsorbed on the sinter of the positive electrode; however, there is no mechanism under the condition of overdischarge to remove the adsorbed hydrogen atoms from the positive electrode.

Combining reactions (5) and (6) yields the equation:

$$H_2 + Cd(OH)_2 \xrightarrow{i_2} Cd + 2H_2O \quad (7)$$

where i_2 is the rate of hydrogen recombination expressed as a current.

The fact that the negative electrode does not exhaust during extensive overdischarge, well beyond the ampere-hours (Ah) of precharge, strongly suggests that the cadmium hydroxide in the negative is being charged chemically by reaction with hydrogen.

If we assume that the overall rate of hydrogen recombination occurs at i_2, then the rate at which hydrogen is consumed expressed as a rate of pressure charge is given by:

$$-\frac{\Delta P}{\Delta t} = \frac{i_1\ RT}{2VF} \quad (8)$$

when $i_1 = i_2$ (overdischarge current = recombination current)

$$\frac{\Delta Pgen}{\Delta t} + \frac{\Delta Precomb}{\Delta t} = 0 \quad (9)$$

and no net pressure rise occurs.

When $i_1 > i_2$, net pressure rise occurs. When $i_1 < i_2$, pressure drop occurs.

Tests were performed prior to this effort with Ni-Cd cells on open circuit pressurized with hydrogen. The results of these tests indicated that pressure decay rate (hydrogen recombination rate) was directly proportional to hydrogen pressure and that an almost twofold increase in hydrogen recombination rate on open circuit occurred as a result of a 10°C temperature. (Based on this data, the energy of activation for open circuit hydrogen recombination was found to be 12 kcal/mole. Tests performed prior to this effort also indicated an increase in hydrogen recombination rate for completely discharged cells whose terminals were shorted over those that obtained an open circuit. This was attributed to the extended surface area (the positive electrode) at the potential of the cadmium electrode (-0.828 volt).

These data suggested that the hydrogen recombination reaction was first ordered with respect to hydrogen pressure which can be expressed by the rate equaton:

$$d \ln P = -kdt \tag{10}$$

where P is hydrogen pressure, k is the rate constant, and t is time. The data also suggested that the hydrogen recombination rate was directly proportional to the electrode area in contact with the active cadmium-cadmium hydroxide material. The rate of recombination on open circuit expressed as a current is given by:

$$I \text{ recomb} = \frac{2\Delta P}{\Delta t} \frac{VF}{RT^{\circ}} \tag{11}$$

substituting numerical values for the constants R and F

$$I \text{ recomb} = \frac{2.63 \times 10^{6} V}{T_{o}} \frac{\Delta P}{\Delta t} \tag{12}$$

where $\Delta P/\Delta t$ = psi per minute.

Current density must be used to compare recombination rate for different cells with different negative electrode surface areas.

The rate of recombination expressed as a current density =

$$ID = \frac{2.63 \times 10^{6} V \frac{\Delta P}{\Delta t}}{T^{\circ} S} \tag{13}$$

where S is total negative electrode surface area at the potential of the negative $Cd/Cd(OH)_2$ electrode.

The hydrogen recombination current density during overdischarge at pressure equilibrium is given by:

$$ID = \frac{I\ overdischarge}{S} \tag{14}$$

The hydrogen recombination current density during overdischarge at non-equilibrium condition:

$$I\ recomb = I\ overdis \pm \frac{2.63 \times 10^6 V \frac{\Delta P}{\Delta t}}{T°} \tag{15}$$

$$ID = \frac{I\ overdischarge}{S} \pm \frac{2.63 \times 10^6 V \frac{\Delta P}{\Delta t}}{T°S} \tag{16}$$

- if $\frac{\Delta P}{\Delta t}$ is positive

+ if $\frac{\Delta P}{\Delta t}$ is negative

3. EXPERIMENTAL PROCEDURE AND DATA

3.1 CONFIRMATION OF HYDROGEN RECOMBINATION MECHANISM

3.1.1 Cell AC Impedance Measurement During Overdischarge

Five new 10 Ah, Ni-Cd cells manufactured by General Electric were fitted with pressure gauges given a 30-cycle conditioning and subjected to overdischarge at 50 milliamperes (C/200). Pressure equilibrium was attained after 10 hours. AC impedance measurements at 60 Hz were taken on open circuit and at various stages of overdischarge. The results in Table 3-1 show no difference in ac impedance during overdischarge and on open circuit. After the overdischarge, cells were given a standard charge retention test which indicated that no cell was shorted. Subsequent to the charge retention test, ac cell impedance was measured at 60 Hz and was somewhat less than during overdischarge. The average cell voltage during overdischarge was -0.100 to -0.200 volt. The results indicate no shorts prior to, after, or during overdischarge in any of the five cells.

Table 3-1. Cell Pressure and AC Impedance Versus Time During Overdischarge at 50 Milliamperes

Time (hr)	Cell Pressure (psia)					Cell Impedance (mΩ)				
	1	2	3	4	5	1	2	3	4	5
10	20	19	19	21	26	2.70	-	-	-	-
15	20	19	19	21	26	2.65	-	-	-	2.60
17	20	19	17	21	26	2.65	-	-	-	2.70
32	19	17	17	20	25	2.65	2.65	2.60	2.45	2.55
35	19	17	16	19	23	2.60	2.60	2.60	2.65	2.50
40	19	17	16	19	22	2.70	2.70	2.67	2.85	2.65
O.C.	19	17	16	19	22	2.70	2.72	2.67	2.84	2.65
After Charge Retention Test										
	-	-	-	-	-	2.40	2.40	2.40	2.64	2.40

3.1.2 Chemical Reduction of $Cd/Cd(OH)_2$ Negative Electrode by Hydrogen

3.1.2.1 Construction of Laboratory Cells

The thickness, flooded capacity, and residual porosity of samples of electrodes used to construct laboratory cells was determined as shown in Table 3-2. The porosity of the separator, pellon 2505K was calculated as 75 percent at a compression to a thickness of 8 mil. The negative electrodes manufactured by G.E. were electrochemically impregnated to the extent of 1.8 gram $Cd(OH)_2$/cc void. The positive electrodes were also fabricated by G.E. but by a vacuum-impregnated process. The positive contained 14.6 g/dm^2 of $Ni(OH)_2$.

Table 3-2. Characteristics of Electrodes Used in Construction of Laboratory Cells

Electrode	Thickness (mm)	Capacity (Ah)	Porosity (%)
Negative	0.78	1.85	50
Positive	0.65	1.68	26

In order to construct negative limiting cells from these electrodes, it was necessary to use eight positive electrodes and five negative electrodes. A separator was inserted between each of two positives and one negative electrode in an accordian wrap. Two such cells were constructed.

The residual void volume of the stack (V.V.S.) is given by the equation:

$$V.V.S. = 5(A_N \times t_N)\rho_N + 8(A_P \times t_P)\rho_P + (A_S \times t_S)\rho_S \qquad (17)$$

where A and t are the electrode/separator area and thickness and ρ is the porosity. Subscripts N, P, and S are positive, negative, and separator.

The interelectrode distance is by definition equal to the thickness of the separator in the cell. In this particular case, the interelectrode distance was 8 mil or 0.020 centimeter. The area of each electrode was 53.2 sq cm^2. The total area of separator used to make this core was 672 cm^2. The average thickness of the positive electrodes was 0.065 centimeter, while the negative electrode thickness was 0.078 centimeter.

Using equation (17) to calculate the residual void volume of the stack

$$V.V.S. = 5(53.2\ cm^2 \times 0.078\ cm)0.50 + 8(53.2\ cm^2 \times 0.065\ cm)0.26 + (672\ cm^2 \times 0.020\ cm)0.75$$

$$V.V.S. = 10.4\ cm^3 + 7.2\ cm^3 + 10.1\ cm^2 = 27.7\ cm^3$$

Each of the two cores constructed were inserted into a cell housing (Figure 3-1) with proper shimming so that the interelectrode distance between each of the two positive and one negative electrodes was 0.20 mm (8 mil). One of the two cells (No. 1) was equipped with a $Cd/Cd(OH)_2$ reference electrode, the other (No. 2) was equipped with a $Ni\ OOH/Ni(OH)_2$ reference. Both cells were equipped with pressure gauges and release valves.

The cells were sealed and, after determining them to be free of shorts and leaks, the cells were weighed and filled with excess electrolyte. The cells were then charged sufficiently to fully charge the positive and negative electrodes. During this charge, the release valve was open, which allowed for draining of excess electrolyte and for the escape of gases produced during overcharge. Both cells were then discharged to 1.0 volt and excess electrolyte removed from the cells by turning them upside down and evacuating with a vacuum pump into a trap as shown in Figure 3-2. The removal of electrolyte by evacuation was repeated until the desired amount of electrolyte remained in the cells. In this case, 37 grams or 27.7 cm^3 was the desired amount. The amount of electrolyte fill of the residual void volume was set at 100 percent which corresponded to 37 grams of electrolyte.

3.1.2.2 Cell Tests

Cells were then subjected to 30 conditioning cycles at a C/4 charge rate for 3 hours followed by a C/2 discharge rate for 1 hour. Following the conditioning cycles, cell No. 1 was evacuated and filled with 50 psig of helium, cell No. 2 was also evacuated but filled with 59 psig of hydrogen. The cells were allowed to stand on open circuit while pressure and negative to reference voltages were monitored.

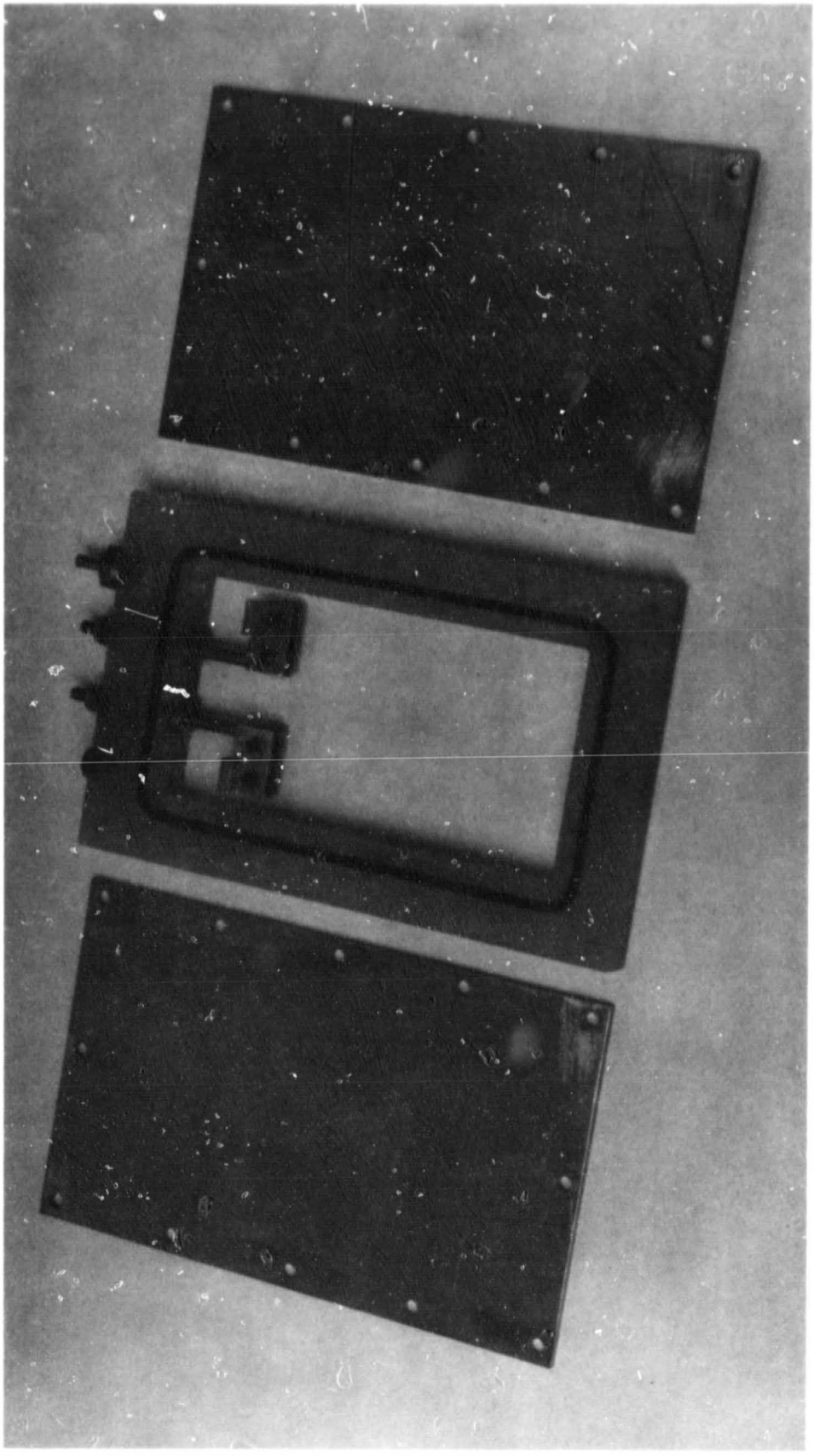

ORIGINAL PAGE
BLACK AND WHITE PHOTOGRAPH

Figure 3-1. Cell Housing for Laboratory Cells

ORIGINAL PAGE
BLACK AND WHITE PHOTOGRAPH

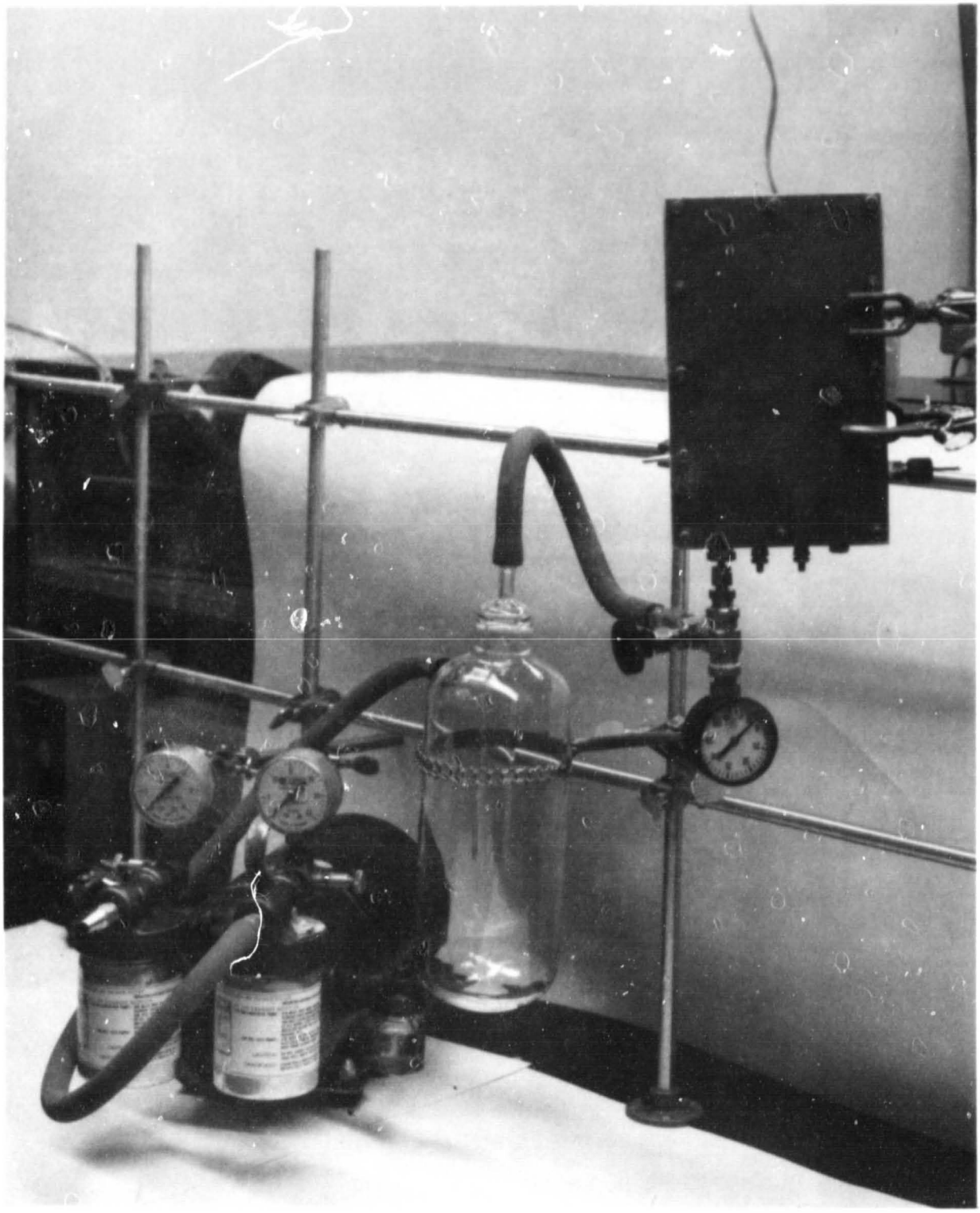

Figure 3-2. Removal of Excess Electrolyte by Exhausting Cell Through Trap

3.1.2.3 Test Results

Figure 3-3 is a plot of negative to reference voltages and cell pressures. The results show no significant change in reference to negative voltage or pressure for cell No. 1 filled with helium over a 1-day period, while cell No. 2 filled with hydrogen showed a pressure decay of 4 psi and a negative to reference voltage increase of more than 0.7 volt. This result indicated the consumption of hydrogen and the simultaneous charge of the negative electrode.

The test was repeated using two of the 10 Ah G.E. cells (mentioned in 3.1.1), which afforded the opportunity to compare hydrogen recombination rates of state-of-the-art cells which contain negatives doped with a small amount of silver and the laboratory cell whose negative did not contain silver.

Figure 3-4 shows a plot of pressure decay for 10 Ah cells filled with hydrogen and helium; again, no significant pressure decay occurred in the helium-filled cell. The rate of pressure decay in the hydrogen-filled 10 Ah cell seems significantly greater than observed for the laboratory cell. However, the void volume of the 10 Ah cell was 30 cc as compared to 50 cc for the laboratory cell and the surface area of the negative was 5.2 dm^2 as opposed to 2.7 dm^2 for the laboratory cell. The recombination rate expressed as a current density normalizes both these effects and the open circuit recombination rate expressed as current density for the 10 Ah cell is not significantly different for the laboratory cell average as shown in Table 3-3.

Table 3-3 compares hydrogen recombination as a current density relative to actual negative electrode surface area in the open-circuit state, during discharge, and during overdischarge. It should be noted that there is an order of magnitude difference between the rate of open circuit hydrogen recombination and recombination rate during discharge, and two orders of magnitude during overdischarge.

The difference between discharge recombination rate and open circuit recombination rate may be due to the polarization of the negative electrode which is more positive during discharge than on open circuit and avails a greater voltage difference between the hydrogen recombination potential and

OF POOR

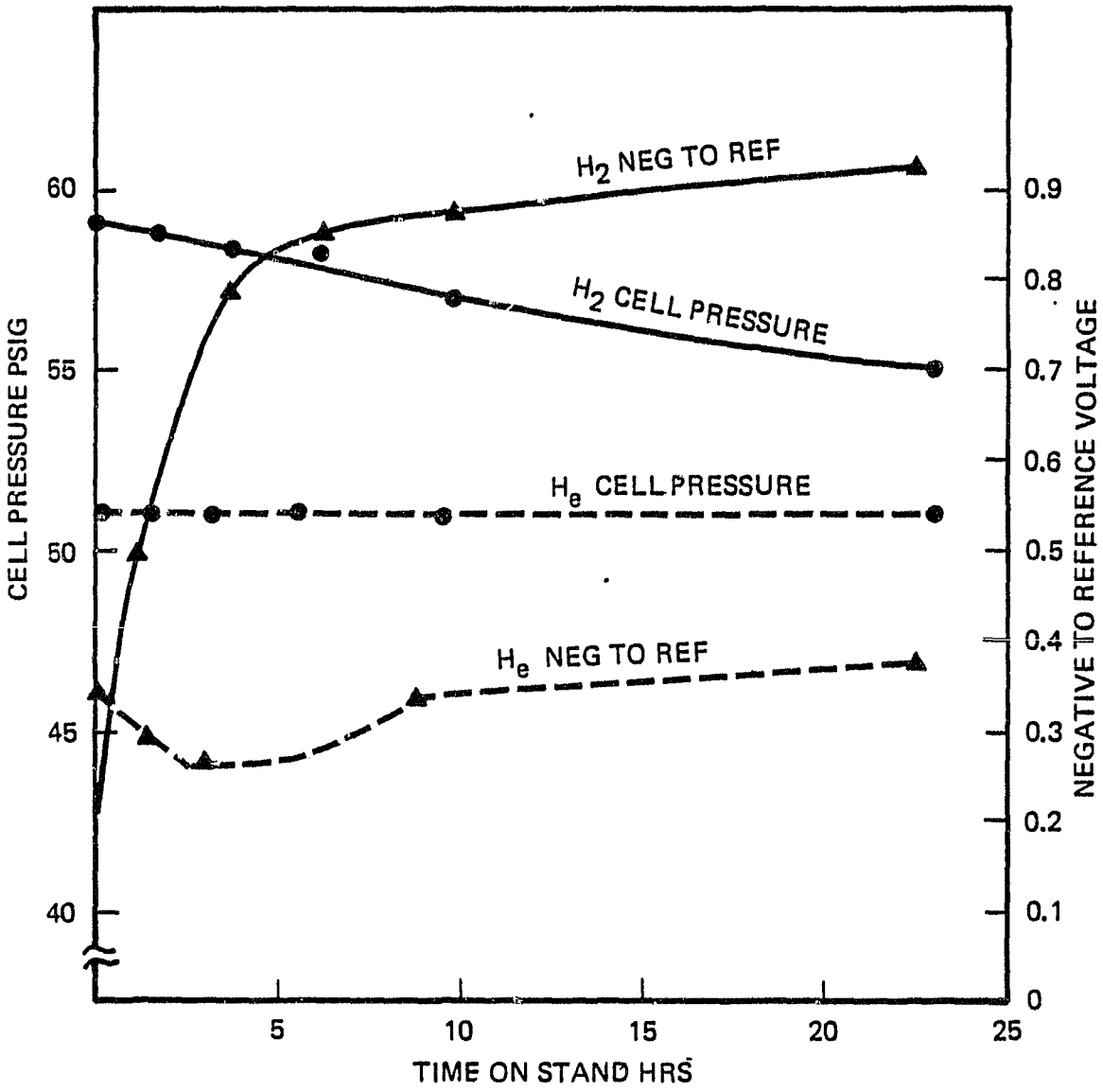

Figure 3-3. Negative to Reference Voltage and Pressure Versus Time for Two Cells: One Containing Helium and the Other Hydrogen

ORIGINAL PAGE IS
OF POOR QUALITY

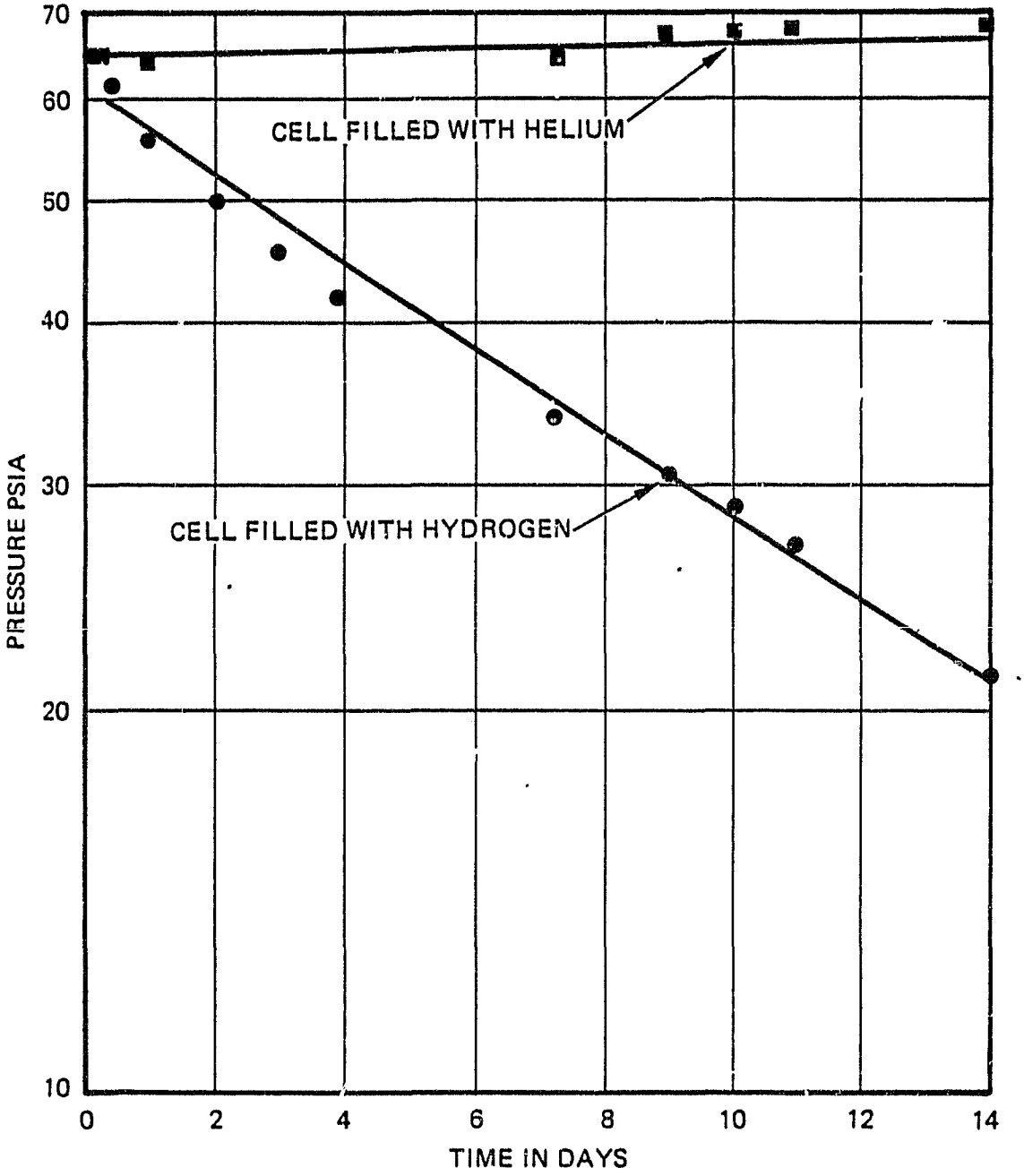

Figure 3-4. Helium and Hydrogen Pressure Decay on Open Circuit for Discharged Positive Limiting Ni-Cd Cells (10 Ah)

Table 3-3. Rates of Hydrogen Recombination Expressed as Current Density (per Unit Negative Electrode Surface Area)

Condition	Cell	Current Density* (mA/dm^2)
Open circuit	Best state-of-the-art Ni-Cd	0.43
	Laboratory Ni-Cd (unoptimized)	0.33
	10 Ah cell	0.23
Discharge	Laboratory cell (unoptimized)	3.0
Overdischarged	Best state-of-the-art Ni-Cd	36.4
	Unoptimized laboratory cell	9.4
	Optimized laboratory cell	93.8

*At pressures of 50 to 80 psia.

the cadmium electrode than an open circuit. The additional increase in recombination rate noted during overdischarge may be related to the tendency of any excess electrolyte to go within the electrodes during reversal* thus reducing the diffusion layer of electrolyte and facilitating hydrogen diffusion to the sinter.

3.1.3 Effect of Temperature and Pressure on Hydrogen Recombination

Three positive limiting cells (No. 3, 4, and 5) each consisting of five positive and six negative electrodes from the same batch as was used in cells 1 and 2 and whose characteristics are described in Table 3-2, were constructed and equipped with a pressure transducer and release valve. Each cell had an interelectrode distance of 8 mil (0.020 centimeter) and its cores residual void volume was 100 percent filled with electrolyte. Precharge was set at 1.8 Ah by venting an appropriate amount of oxygen (70 psi for a void volume of 82 cc). The cells were 6 Ah in capacity and were subjected to 30 cycles of conditioning at a C/4 rate for 3 hours and a C/2 discharge rate for 1 hour prior to initiation of testing.

After completion of conditioning, the three cells were completely discharged. Each was filled with hydrogen at 30, 60, and 90 psia and overdischarged for a period of 3 hours at C/100 (60 milliamperes) for each pressure setting.

*This was observed independently of the author in 1958 and by H. N. Seiger in 1956 during the overdischarge of flooded Ni-Cd cells.

Table 3-4 lists the pressure increases observed as well as the average pressure during each 3-hour overdischarge period.

Using equation (15)

$$I_{\substack{\text{hydrogen}\\\text{recombination}}} = I_{\text{overdischarge}} - \frac{2.63 \times 10^6 (V)}{T^\circ} \frac{\Delta P}{\Delta t}$$

where $\Delta P/\Delta t$ = psi/min.

Table 3-4. Observed Pressure Increase and Average Pressure During 3-Hour Overdischarge

	Cell 3		Cell 4		Cell 5	
	Increase (psi)	Avg (psia)	Increase (psi)	Avg (psia)	Increase (psi)	Avg (psia)
Test 1	12.0	35	10.0	60	8.7	63
Test 2	9.7	65	7.6	88	6.6	92
Test 3	6.9	95	9.0	39	7.2	35

The hydrogen recombination current was calculated for each condition for each cell is shown in Table 3-5. The number in parentheses represents the sequence of the test, which is significant as will be explained in the following paragraphs.

Figure 3-5 shows a plot of average cell pressure versus hydrogen recombination rate for the three cells. Note that all three data points for cell 3 fall on a straight line which passes through zero. Two data

Table 3-5. Hydrogen Recombination Current (Milliamperes) During Overdischarge at Various Pressures of Hydrogen

Nominal Initial Pressure (psia)	Cell 3	Cell 4	Cell 5
30	13.9(1)	25.3(3)	32.2(3)
60	22.6(2)	21.5(1)	26.5(1)
90	33.5(3)	30.8(2)	34.6(2)

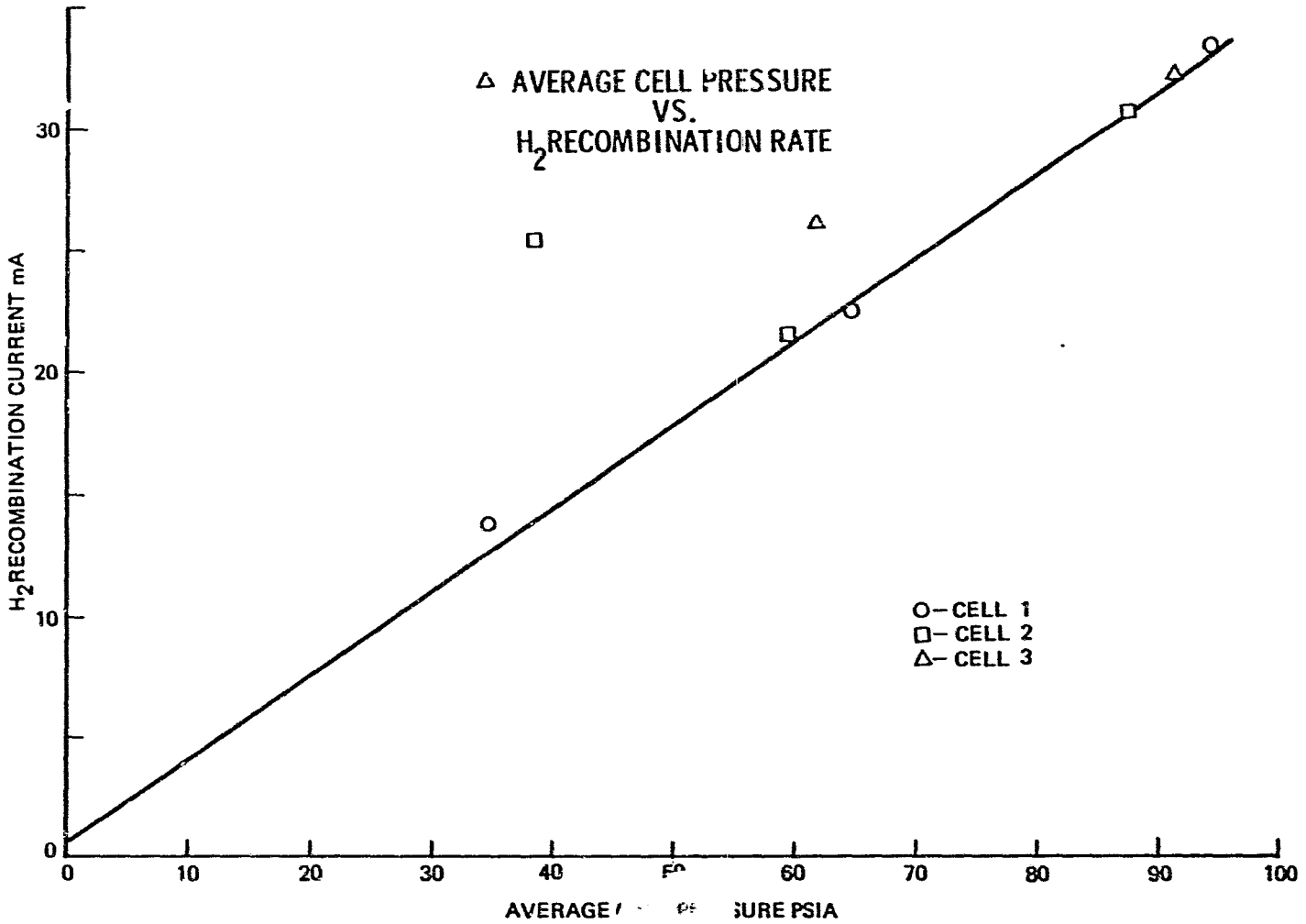

Figure 3-5. Effects of Pressure on Hydrogen Recombination Rate During Overdischarge

ORIGINAL PAGE IS OF POOR QUALITY

points for each of cells 4 and 5 either fall on that line or are close to it. The data indicates the direct linear relationship between pressure and hydrogen recombination rate during overdischarge. Two of the nine data points are significantly removed from the linear plot. Rather than consider these to be random error in the data, these points are a result of test sequence. Cell 3 was tested in the sequence 30, 60, and 90 psia. The test sequence of cells 4 and 5 were 60, 90, and 30 psia. The two points not on the straight line in Figure 3-2 are the 30 psia test for both cells 4 and 5. These data suggested that sequential testing increases the rate of hydrogen recombination. To verify this, the overdischarge at 30 psia was repeated for cell 5. The recombination rate during this test was 41.9 milliamperes as opposed to 34.6 milliamperes found on the test just before. There was no further tests made to quantize the sequence effect and calibrate the data.

The effect of temperature on hydrogen recombination was studied using the same three cells as used for the pressure experiment above. Cells 3, 4, and 5 were each pressurized with hydrogen at 60 psia and overdischarged for 3 hours at 5, 10, and 20°C at a current of 60 milliamperes.

Using equation (15)

$$I_{recomb} = I_{OD} - \frac{2.63 \times 10^{6} V}{T^{\circ}} \frac{\Delta P}{\Delta t}$$

to calculate recombination current, the data shown in Figure 3-6 was generated. Figure 3-6 is a plot of recombination rate versus average pressure for three cells at three temperatures. Neglecting the effect of sequence which was 5°C, then 10°C, and finally 20°C, the energy of activation was determined by plotting the natural log within the reaction rate which is directly proportional to rate constant against the reciprocal of the absolute temperature as shown in Figure 3-7. The energy of activation for active hydrogen recombination (hydrogen recombination during overdischarge) was found to equal 2.8 kcal/mole which is about 0.2 of the value found for open circuit stand hydrogen recombination. If the sequence effect is taken into consideration, the apparent energy of activation could be as low as zero. At present there is no explanation of this apparent anomaly.

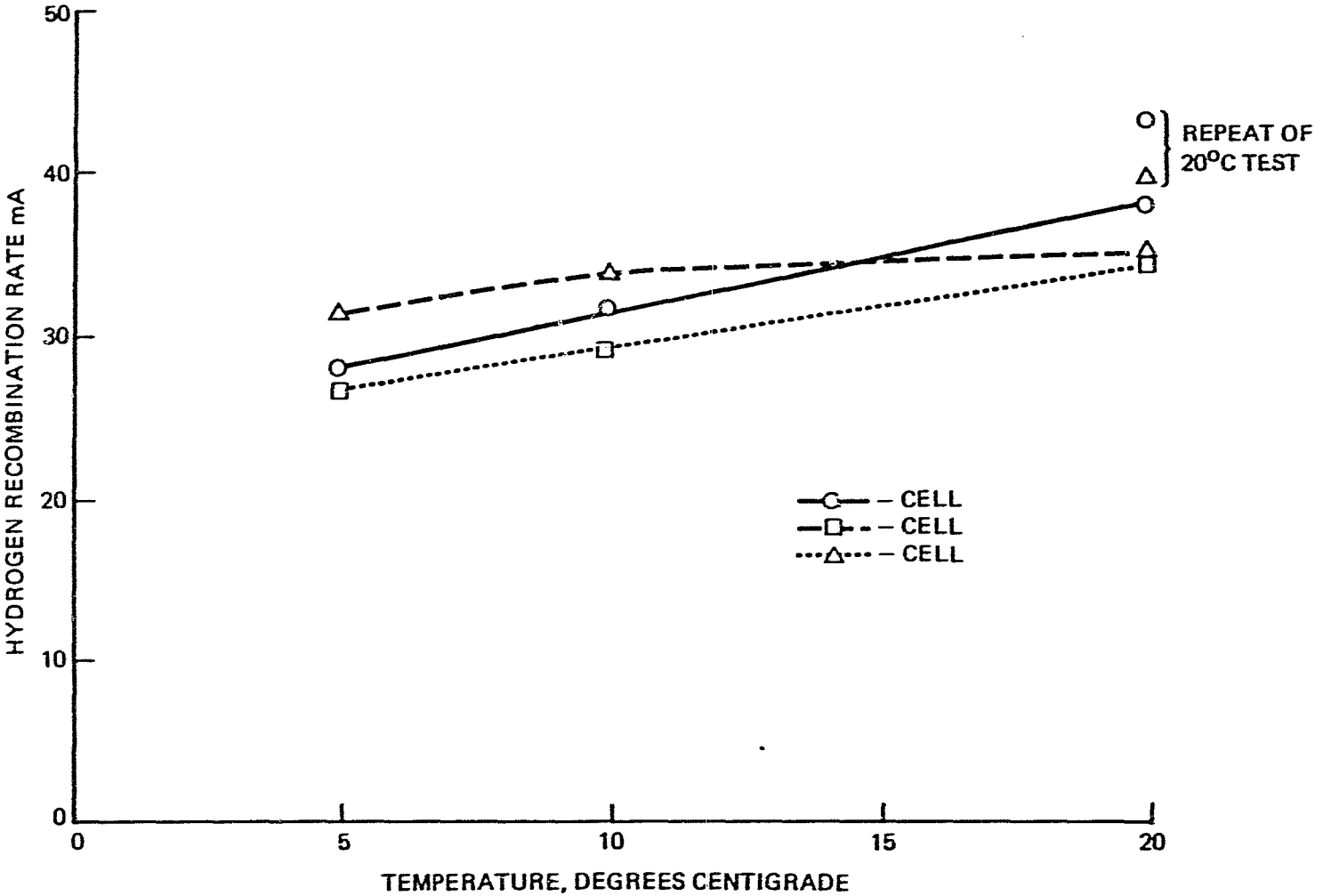

Figure 3-6. Effects of Temperature on the Hydrogen Recombination Rate During Overdischarge

OF POOR QUALITY

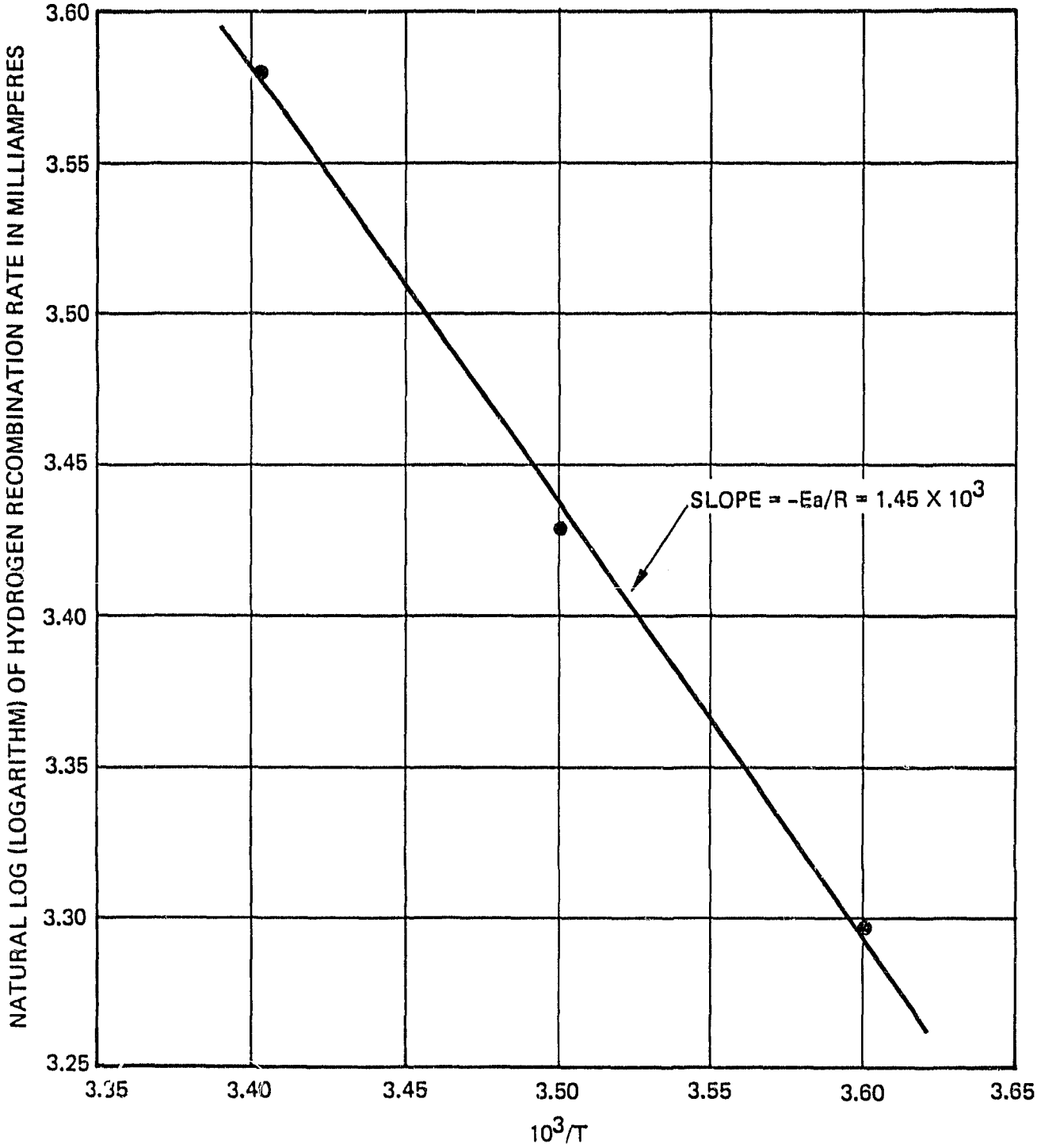

Figure 3-7. Natural Logarithm Hydrogen Recombination Rate Versus Reciprocal of Absolute Temperature

3.2 PARAMETRIC CELL DESIGN STUDY

A parametric design study was undertaken with the objective of developing a nickel-hydrogen cell with improved (increased) hydrogen recombination capability.

3.2.1 Experimental Design - Parametric Study

Thirty-six Ni-Cd cells representing 18 different cell designs at a replication of two were constructed. The 18 different designs varied with respect to: (1) method of negative electrode impregnation, (2) electrolyte concentration, (3) electrolyte fill of residual core void volume, (4) negative precharge, and (5) interelectrode distance. The experimental design and the different values assigned to these parameters are shown in Table 3-6.

In addition to the five parameters, a sixth, the extent of active material loading of the negative electrode was investigated. Six cells identical with respect to the five parameters of Table 3-6 but different with respect to active material loading of the negative electrode were used for this study.

3.2.2 Test Cell Construction

All test cells were positive limiting, contained six negative and five positive electrodes had a nominal capacity of 6 Ah, and contained a NiOOH/$Ni(OH)_2$ reference electrode and were equipped with valves and pressure transducers. The electrodes for 18 of the cells were identical to those used in previous tests described in this report. Eighteen other cells contained the same positive electrode as described before but instead of electrochemically impregnated negative, these cells had vacuum-impregnated negatives loaded to 2.3 grams of $Cd(OH)_2$ per cubic centimeter of void. Four additional cells were made with the same positive but electrochemically impregnated negative, two cells with a negative electrode loading of 2.1 g/cm^3 void and two with negative loading of 1.4 g/cm^3 void. Cell were constructed using the techniques described in Section 3.1.2 to set interelectrode distances, establish electrolyte filling of residual void volume and set precharge.

Table 3-6. Parametric Experiment Design

METHOD OF NEGATIVE ELECTRODE IMPREGNATION	PRECHARGE (%)	ELECTROLYTE CONCENTRATION (%KOH)	ELECTROLYTE FILL = 80%			ELECTROLYTE FILL = 100%		
			INTERELECTRODE DISTANCE (mil)			INTERELECTRODE DISTANCE (mil)		
			4	6	8	4	6	8
ELECTROCHEMICAL	40	32	—	n = 2	n = 2	—	n = 2	n = 2
	20	28	n = 2	—	—	—	—	—
		32	—	n = 2	n = 2	—	n = 2	n = 2
VACUUM	40	32	—	n = 2	n = 2	—	n = 2	n = 2
	20	28	n = 2	—	—	—	—	—
		32	—	n = 2	n = 2	—	n = 2	n = 2

n = NUMBER OF CELLS

Table 3-7 lists the 18 cells, beginning with cell 6 made with electrochemically impregnated negative electrodes and lists their parametric design characteristics.

A similar list appears later in the text for the 18 cells made with vacuum-impregnated negative electrodes.

Table 3-7. List and Design Characteristics of Cells Made with Electrochemically Impregnated Negative Electrode

Cell No.	Interelectrode Distance (mil)	Electrolyte Fill Percent of Residual Porosity	Electrolyte Concentration (Percent)	Precharge Percent in Excess of Nominal Cell Capacity
6, 7	6	100	32	40
8, 9	8	80	32	40
10, 11	8	100	32	20
12, 13	6	100	32	20
14, 15	6	80	32	20
16, 17	6	80	32	40
18, 19	8	100	32	40
20, 21	8	80	32	20
22, 23	4	80	28	20

3.2.3 Experimental Tests

3.2.3.1 Electrochemically Impregnated Negatives

Following 30 conditioning cycles, testing of cells commenced. Initial testing was performed with the 18 cells containing electrochemically impregnated negative electrodes. Each of these cells was subjected to sequential overdischarge rates of C/100, C/50, C/20, C/5, and C/2 (0.060, 0.120, 0.300, 1.2, and 3.0 amperes, respectively). The initial overdischarge rate 60 milliamperes was applied to each cell until pressure equilibrium was attained or cell pressure reached 120 psia.

If a cell failed to reach equilibrium prior to reaching 120 psia, the cell was removed for further testing. If a cell went to undervoltage, (more negative than -0.5 volt) indicating exhaustion of precharge prior to reaching equilibrium or 120 psia, the precharge was reset and the test

repeated. Cells which attained equilibrium during the 60-milliampere overdischarge were permitted to be overdischarged at 120 milliamperes. Prior to beginning the overdischarge at 120 milliamperes, any hydrogen pressure left in the cell had to be evacuated. The Ah equivalent of the evacuated hydrogen corresponds to a loss of some of the precharge of the negative in test cells.

Precharge lost through the evacuation of unrecombined hydrogen was restored to the cell by overcharging and venting the appropriate amount of oxygen. (For every psi of hydrogen evacuated, 0.5 psi of vented oxygen restores the precharge lost.)

At 120 milliamperes, the limitations on the cell were the same and those cells which passed these criteria were allowed to go on and be overdischarged at 300 milliamperes after adjustment in hydrogen pressure and precharge were made. None of the 18 cells could be overdischarged beyond 300 milliamperes without achieving overpressure or undervoltage.

The cells which could sustain the greatest overdischarge current were numbers 6 and 7, both of the same design. The cell's design was:

Interelectrode distance	6 mil
Electrolyte fill	100 percent
Electrolyte concentration	32 percent
Precharge	40 percent
Impregnation of negative	electrochemical
Loading	1.8 g/cm^3 void

Figure 3-8 is a plot of recombination rate versus equilibrium pressure for cells 6 and 7. Note that the plot is linear and when extrapolated passes through zero, in agreement with the hydrogen recombination mechanism.

3.2.3.2 Effect of Negative Electrode Active Material Loading

After establishing that particular design as optimum for hydrogen recombination for cells made with electrochemically impregnated negatives, four additional cells of that design were tested. Two of the cells, however, were made with electrochemically impregnated positives loaded to 1.4 g/cm^3 void and two others with a negative loading of 2.1 g/cm^3 void. Thus, six cells counting the two with 1.8 g/cm^3 void loading previously made (cells 6 and 7) were available for comparison with respect to active

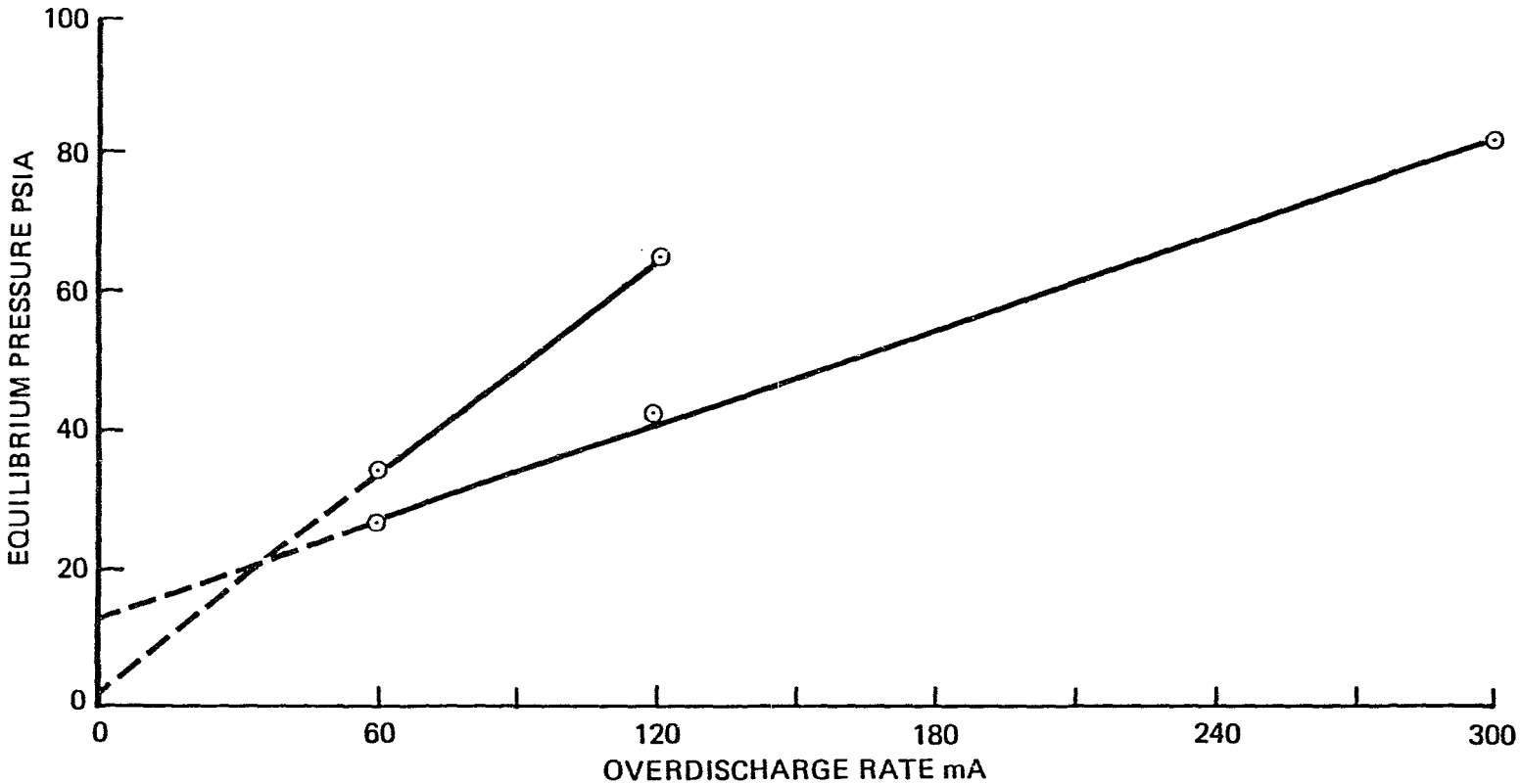

Figure 3-8. Equilibrium Pressure Versus Overdischarge Rate for Two Cells of Optimum Design Made with Electrochemical Impregnated Negative Electrodes

material loading of the negative effect on the hydrogen recombination rate. The comparison performed as described for the parametric test above resulted in the 1.4 g/cm^3 negative loaded cells giving the best recombination rate and the 2.1 g/cm^3 void and the worst.

Cells 24 and 25 made with negative electrodes loaded to 2.1 g/cm^3 void were able to sustain an overdischarge rate at 120 milliamperes but reached overpressure and 100 psia equilibrium pressure at 300 milliamperes. Cells 26 and 27 containing negative electrodes loaded to 1.4 g/cm^3 void both sustained a 300-milliampere overdischarge reaching equilibrium pressures of 40 and 35 psia, respectively. The overdischarged capability of cells 6 and 7 with negatives loaded at 1.8 g/cm^3 void was listed in the previous section. The results of these tests indicate that cells made with negative electrodes loaded to 1.4 g/cm^3 void gave the best hydrogen recombination capability.

Results on the effect of loading obtained with electrochemically impregnated negatives indicated that a 1.4 g/cm^3 loading gave the best hydrogen recombination capability; however, as will be shown below, such a loading would result in a weight increase of about 20 percent. Consider a 20 Ah lightweight Ni-Cd cell weighing 550 grams. Assume that the number of negative electrodes can be increased to accommodate the decreased loading while maintaining total weight of $Cd(OH)_2$ and total weight of the positive electrodes a constant. Table 3-8 shows effect of loading level on total negative electrode weight.

Table 3-8. Effect of Loading Level of Negative Electrode on Total Negative Electrode Weight

Loading Level		Total Negative Characteristics			
g/cm^3 Void	g/dm^2 at 82 Percent Porosity	Weight $Cd(OH)_2$(g)	Total Void Volume (cm^3)	Sinter Weight (g)	Total** Weight (g)
2.1	13.7	130	62	121	251
1.8	11.7	130	72	141	271
1.4	9.1	130	93	182	312

In order to accommodate the decreased loading, the number of negative electrodes must increase. Thus, if there were nine negative electrodes in the cell at a negative loading level of 13.7 g/dm^2, 11* and 14* electrodes are required at loading levels of 11.7 and 9.1 g/dm^2. (The number and weight of positive electrodes would remain constant. This is achieved by placing some of the negative electrodes back to back.) Assuming a negative electrodes thickness of 0.031 inch an increase of two and five electrodes results in a cell thickness increase of 0.062 and 0.151 inch, respectively. For an 0.012-inch cell case with dimensions of 4.5 by 3.0 by 1.0 inches, the weight increase due to increase in thickness equals 0.3 and 0.8 gram, respectively. The additional number of electrodes increases the residual void volume to be occupied by electrolyte, as shown in Table 3-9.

Table 3-9. Effect of Loading Level of Negative Electrodes on Electrolyte Weight

Loading Level		Residual Void Volume (After Impregnation)	Weight of Electrolyte in Negative Electrodes at 100 Percent Fill (g)
g/cm^3 Void	g/dm^2 at 82 Percent P		
2.1	13.7	35.0	46.6
1.8	11.7	47.2*	62.8*
1.4	9.1	68.3*	91.0*

*Based on 11 and 14 negative electrodes.

*Calculation corresponds to 10.5 and 13.5 electrodes, adjusting to 11 and 14 electrodes results in an additional weight increase of 14 and 11 grams, respectively.

**Disregarding weight of grid.

The weight increase as a result of loading level decrease considering both effect on electrolyte, electrodes and cell case is 51* and 117* for loading levels of 1.8 g/cm^3 void and 1.4 g/cm^3 void, respectively. For a cell that weighs 550 grams (with a 2.1 g/cm^3 void loading), the percent increase in weight corresponds to 9.2 percent** and 21.2 percent** for negatives loaded to 1.8 g/m^3 void and 1.4 g/cm void, respectively. The choice of 1.8 g/cm^3 void loaded negative is based on the above weight calculations. A loading level of 1.4 g/cm void results in too great a weight penalty.

3.2.3.3 Vacuum-Impregnated Negative Electrodes

The other 18 cells containing vacuum-impregnated negatives are listed and their parametric design described in Table 3-10. These cells, designated 28 to 45, were given 30 conditioning cycles and tested sequentially at overdischarge rates of C/100, C/50, C/20, C/5, and C/2. These cells showed an extraordinary overdischarge capability; in fact, ten of the 18 cells indicated hydrogen recombination rate as great as C/2(3A). The ten cells are listed in Table 3-11 along with equilibrium pressure and total Ah of overdischarge. Table 3-11 lists the ten cells which exhibited the high rate apparent hydrogen recombination capability, their equilibrium pressure and total Ah of reversal at each overdischarge rate.

Because of the unusually high overdischarge rates, these cells were checked for shorts and leaks following the last overdischarge. None of the cells indicated either. Sample cells were subjected to destructive physical analysis including electron microscopy and surface area measurements of the negative electrode by B.E.T. and double layer capacitance to determine if the high recombination rate were due to anything other than the six parameters studied.

---

* Based on 11 and 14 negative electrodes.

** Based on same utilization for all loadings; if utilization as a function of loading levels were taken into consideration weight increases would be approximately 5 and 16 percent for cells made with 1.8 and 1.4 g/cm^3 loaded negatives.

Table 3-10. List and Design Characteristics of Cells Made with Vacuum-Impregnated Negatives

Cell No.	Interelectrode Distance (mil)	Electrolyte Fill Percent of Residual Porosity	Electrolyte Concentration (Percent)	Precharge Percent in Excess of Nominal Cell Capacity
28, 29	8	80	32	20
30, 31	8	80	32	40
32, 33	8	100	32	20
34, 35	8	100	32	40
36, 37	6	80	32	20
38, 39	6	80	32	40
40, 41	6	100	32	20
42, 43	6	100	32	40
44, 45	4	80	28	20

Table 3-11. Cells Capable of Sustaining C/2 Overdischarge, With Equilibrium Pressures (PSIA) Listed at the Various Rates of Overdischarge, and Total Ah of Reversal at Each Rate

Cell No.	60 mA (3 Ah)	120 mA (3 Ah)	300 mA (7.2 Ah)	1.2 A (16.8 Ah)	3.0 A (24.0 Ah)
29	21	6	17	13	30
30	14	2	2	1.7	3.7
31	19	8	16	35	19
32	17	7	4	69	46
36	12	16	9	53	104
37	17	7	4	11	27
38	16	2	2	7	14
39	4	4	6	35	8
42	17	9	13	6	7
45	4	8	5	43	53

3.2.4 Special Tests to Determine Cause of High Overdischarge Capability of Cells Made with Vacuum-Impregnated Negative Electrodes

An additional task was added to the parametric cell design study involving the teardown analysis of three cells which exhibited the high overdischarge rate capability along with one cell which gave standard C/100 overdischarge capability.

These cells were subjected to the following tests:

1 - Electrolyte distribution

2 - Positive and negative electrode physical characteristics

3 - Total cadmium (chemical) contained in the negative electrode

4 - Total silver in the negative electrode

5 - Undischargeable cadmium in the negative electrode

6 - Surface area of the negative electrode by B.E.T. and double layer capacitance method

7 - Determination of trace material in the negative electrode

8 - Surface appearance of the negative electrode via electron microscopy

3.2.4.1 Electrolyte Distribution, Electrode Characteristics and Capacity Tests

Three laboratory cells (29, 39, and 42) which had exhibited hydrogen recombination as high as C/2 and cells which had a recombination rate maximum of C/100 were subjected to teardown. Prior to teardown, the negatives of cell 29 were chemically discharged by overnight exposure to oxygen gas from a tank. The 3 Ah of precharge were returned to the cell by overcharging and venting oxygen. The cell was then completely discharged.

Cells 39 and 42 and the G.E. 15 Ah cell were torn down in the discharged state without further treatment. The results of the teardown which involved electrode thickness measurement, electrolyte distribution in separator, positive and negative electrode capacity, total cadmium in the negative and undischargeable cadmium in the negative, are shown in Table 3-10.

The data summarized in Table 3-12 indicates a slightly drier separator for the high recombination cell and also a slightly greater amount of undischargeable cadmium. It should be noted that the 3 Ah of cadmium precharge put into cell 29 showed up as 2.8 Ah of undischargeable cadmium. Other than the difference in separator wetness and undischargeable cadmium which was higher for the high recombination cells that for the state-of-the-art cells. nothing to account for the high recombination rate was indicated.

3.2.4.2 Chemical Analysis by Mass-Spectroscopy

Samples of the negative electrode from each of the four cells were analyzed by means of mass spectroscopy. The results of that analysis is shown in Table 3-13. Silver, which could have a possible catalytic effect on hydrogen recombination, was less in the negative of the high recombining cells than in the standard cell. Other than that, the table does not reveal the presence or absence of any constituent that could account for the observed high rate overdischarge capability.

3.2.4.3 Microscopy

The negative electrodes from each of the four cells were examined at 2000X magnification with the electron microscope. Photographs are shown in Figures 3-9 and 3-10. The photographs indicate a more open structured surface for the negative of the high recombining cells than found on the structure of the negative for the "normal" recombining cell.

3.2.4.4 Surface Measurements

3.2.4.4.1 Double-Layer Capacitance

Double-layer capacitance measurements were made on an unimpregnated nickel sinter, samples of negative electrodes from the G.E. cell, and negative electrode samples of each of the three cells which exhibited the high recombination rate. The basic principle behind the test is that by superimposing a short-duration voltage pulse over a fixed applied voltage in a noncoulombic range, the double-layer perturbation caused by the pulse is disturbed and then relaxed to be disturbed again by the next pulse. The relaxation on discharge of the double layer caused by the pulse is directly proportional to the magnitude of the pulse and the true surface area of the electrode.

Table 3-12. Teardown Analysis Cell Data for High Recombination Rate Cells and State-of-the-Art Cell

Cell No.	Electrolyte Distribution (g/dm^2)			Electrode Thickness (mil)		Electrode Flooded Capacity (Ah)		Undis* Cd Ah	Total $Cd(OH)_2$ g/dm^2
	Positive	Negative	Separator	Positive	Negative	Positive	Negative		
29	3.4	3.6	0.6	32.0	32.0	1.6	2.4	2.8	17.2
39	3.1	3.5	0.4	-	32.0	1.5	2.0	2.1	17.5
42	2.7	4.2	0.9	-	33.0	1.6	2.6	3.8	16.5
15 Ah GE	2.3	3.5	1.2	31	31.7	1.6	2.1	1.5	16.6

Table 3-13. Composition of Negative Electrodes in Parts per Million as Analyzed by Mass Spectroscopy

	Cell No.	26	35		38		15 Ah GE	
	N_1	N_2	N_1	N_2	N_1	N_2	N_1	N_2
Ni^-	1900	1700	1500	1800	1600	1700	1000	1400
Cd^-	1400	1700	2000	1500	2000	1600	1700	1700
Cu^-	1.1	1.0	0.60	0.74	0.81	0.95	0.82	0.63
B^-	0.45	0.30	0.50	0.40	0.44	0.34	0.42	0.44
Si^-	1.6	0.97	2.1	14.0	2.5	4.7	4.5	4.6
Fe^-	0.55	0.56	0.60	0.79	0.83	0.49	0.62	1.0
Mg^-	0.86	0.42	0.70	0.58	0.34	0.71	0.81	1.8
Al^-	0.46	0.45	0.75	0.48	0.75	0.87	0.74	1.1
Ag^-	<0.01	<0.01	<0.01	<0.01	0.025	0.023	0.041	0.043
Na^-	6.3	8.3	17.0	9.5	19.0	16.0	14.0	19.0
Ca^-	0.51	0.41	1.6	1.1	1.1	1.5	1.2	2.0
Cr^-	<0.01	<0.01	0.018	0.032	0.030	0.029	7.001	0.023
Other Elements	mil	mil	mil	mil	mil	mil	mil	mil
Loss on Ignition	99.24%	99.24%	99.23%	99.25%	99.22%	99.26%	99.27%	99.30%

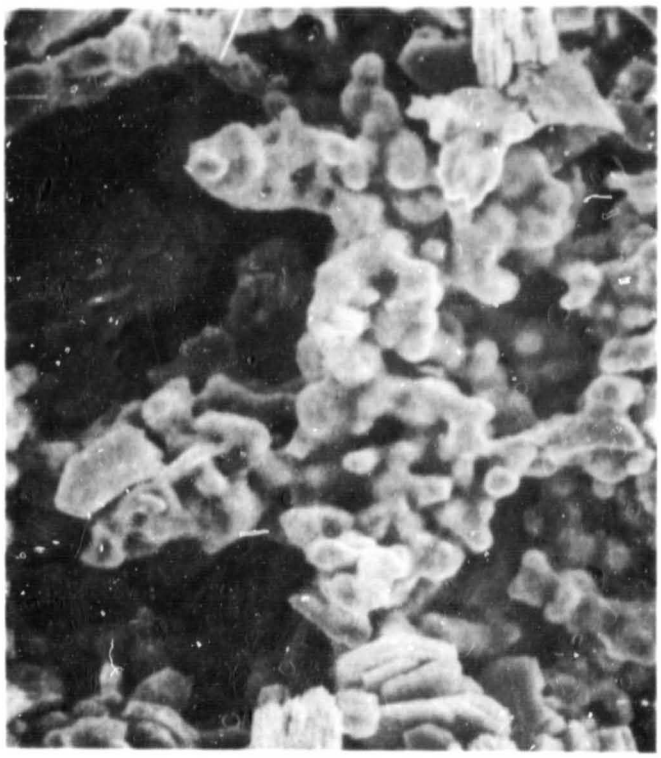

Cell 26 Negative

Cell 35 Negative

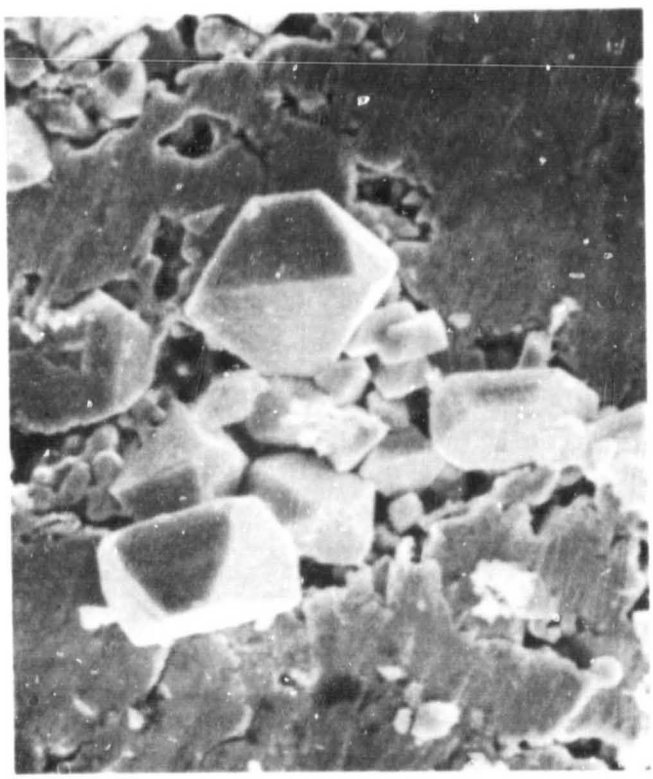

15 Ah GE Cell Negative

Figure 3-9. Electron Microscope Photos of Negative Electrodes at 2000X Magnification

ORIGINAL PAGE
BLACK AND WHITE PHOTOGRAPH

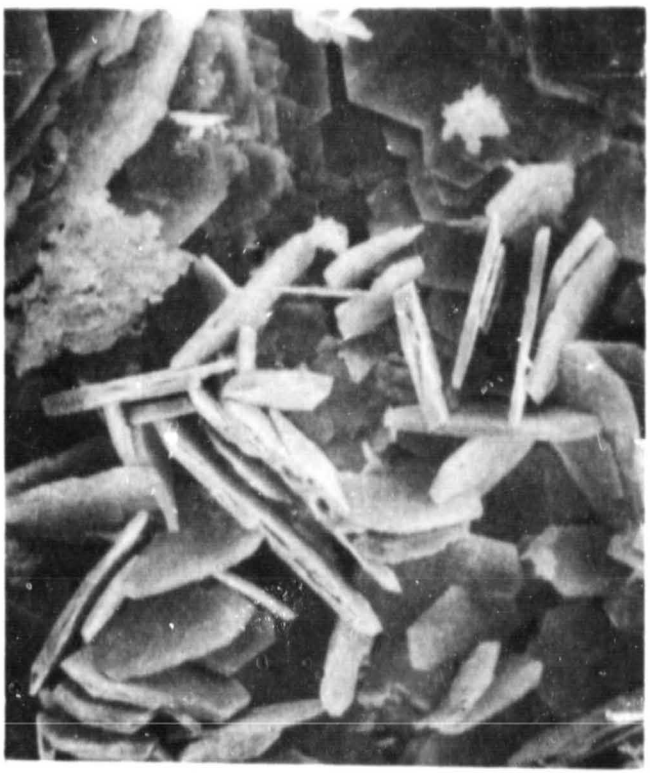

Cell 38 Negative

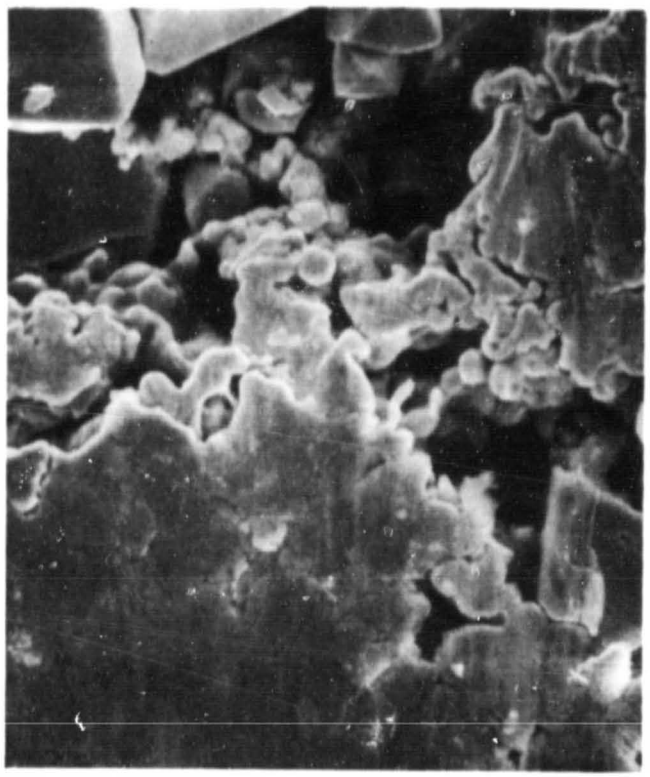

15 Ah GE Cell Negative

Figure 3-10. Electron Microscope Photos of Negative Electrodes at 2000X Magnification

ORIGINAL PAGE
BLACK AND WHITE PHOTOGRAPH

By comparing coulombs of double-layer discharge at a fixed voltage and a fixed pulse for different electrodes, a comparison of their true surface area can be made. The surface area of a sintered unimpregnated plaque end of the various negative electrodes was calculated from double-layer capacitance measurements. Unit surface capacitance is given by the equation:

$$\bar{c} = \frac{1}{A\Delta E} \int_0^t i dt$$

where

$\bar{c}$ = unit surface capacitance

i = capacitance discharge current

A = electrode geometric area

t = time of capacitance discharge

ΔE = pulse voltage

The specific capacitance of a nickel surface is defined as the capacitance of true surface (time surface is twice the geometric area and is equal to 20 $\mu F/cm^2$, a standard reference value.

Table 3-14 lists the various electrodes where double-layer capacitance was measured, their weight, geometric area, double-layer capacitance, capacitance per cm^2 of geometric area, and capacitance per gram. The values of surface area per gram for all the negative electrodes tested ranged from 850 to 920 cm^2/g. These values were obtained by dividing the value of the double-layer capacitance per gram by one half of the specific capacitance (the specific capacitance value is for the total surface which represents twice the geometric area).

The value for the surface area for the unimpregnated sintered plaque was calculated as 840 cm^2/g. This is in excellent agreement with literature values for Heliotek plaque. ("Double Layer Capacitance of Porous Nickel Electrode by Square Wave Pulse Techniques" Seiger, Yao, Puglisi and Bene.)

ORIGINAL PAGE IS
OF POOR QUALITY

Table 3-14. Double Layer Capacitance (DLC) Data for Sinter and Various Negative Electrodes

Electrode	Weight (g)	Geometric Area (cm^2)	Double Layer Capacitance (μF)	DLC/cm^2 (μF/cm^2)	DLC/g (μF)	1/2 Standard Value for Smooth Ni Surface (10 μF/cm^2)
Sinter	8.5	53	7.4×10^4	1.4×10^3	8.4×10^3	10 μF/cm^2
15 Ah GE cell negative	16.4	53	14.8×10^4	2.8×10^3	9.0×10^3	10 μF/cm^2
Laboratory cell No. 26 negative	16.0	44	14.7×10^4	3.3×10^3	9.2×10^3	10 μF/cm^2
Laboratory cell No. 35 negative	15.0	44	12.8×10^4	2.9×10^3	8.5×10^3	10 μF/cm^2
Laboratory cell No. 38 negative	16.0	44	14.7×10^4	3.3×10^3	9.2×10^3	10 μF/cm^2

3.2.4.4.2 B.E.T. Gas Absorption Technique

Surface areas of negative electrode test sample were also measured by B.E.T. gas absorption technique. This measurement was performed by the Analytical Chemistry Group. For their particular setup, the plate sample had to lose their structural integrity, resulting in surface area values which were more than an order of magnitude greater than the double-layer capacitance surface area value and about an order of magnitude greater than literature values for measurement of these surfaces by the B.E.T. technique. The results of these measurements are shown in Table 3-15 and range from 2.04 m^2/g to 5.63 m^2/g. The difference between the surface area of the negative of a standard recombination cell and the negative of the high rate recombining cells is at most twofold which does not account for the 50-fold increase in hydrogen recombination capability.

Table 3-15. Surface Area per Gram of Negative Electrode as Measured by BET Gas Absoprtion Technique

Negatives From Cell No.	Surface Area (cm^3/g)
29	25,300
29	20,900
39	29,900
39	20,400
42	56,300
42	35,000
G.E. 15 Ah	25,700
G.E. 15 Ah	21,600

In both the double-layer capacitance and B.E.T. measurement of surface area, the difference between values of surface area obtained is by far not enough to account for the almost two orders of magnitude difference in hydrogen recombination rate.

Except of electrolyte distribution, silver content and crystal time size and shape no significant difference was found at the completion of testing to determine if any significant difference exists between the negative electrodes which resulted in cells with a hydrogen recombination rate of C/2 and so called state-of-the-art electrode. It was decided to cease further testing and to order negative electrodes with a loaded level of 11.7 g/dm^2 (1.8 g/cm^3 void) made by vacuum impregnation from General Electric for the construction of 14 identical cells of optimum hydrogen reconstruction.

3.3 DESIGN, CONSTRUCTION, AND EVALUATION OF CELLS WITH OPTIMUM HYDROGEN RECOMBINATION CAPABILITY

3.3.1 Choice of Design

The optimum recombination capability of C/2 was demonstrated by ten cells, however, only three different cell designs had both cells of that design exhibit the C/2 hydrogen recombination rate. These designs are shown in Table 3-16. From these three designs, a composite design was chosen which has the characteristics shown in Table 3-17.

Table 3-16. Cell Designs Yielding Maximum Hydrogen Recombination Rate

Impregnation Method Negative Electrode	Vacuum	Vacuum	Vacuum
Precharge (%)	40	40	20
Electrolyte Concentration (%)	32	32	32
Electrolyte File (%)	80	80	80
Interelectrode Distance (mil)	6	8	6

Table 3-17. Composite Optimum Cell Design

Interelectrode Distance = 8 mil
Precharge = 40 percent
Electrolyte Fill = 80 percent
Electrolyte Concentration = 32 percent
Negative Electrode
Impregnation - vacuum
Negative Loading = 1.8 g/cm^3

The rationale for using 8 mil instead of 6 mil was because positive electrodes tend to swell during cycling, drying the separators then beginning with an interelectrode distance of 6 mil could result dry separator I.R. voltage losses and poor cell capacity within a few seasons of cycling. The choice of 40-percent precharge over 20 percent was made because it would allow for a greater hydrogen pressure buildup percentage without exhaustion of precharge. The choice of 1.8 g/cm^3 void loading level for the negative electrode was a compromise between hydrogen recombination capability and specific energy. All three designs in Table 3-16 had vacuum-impregnated negative, 32 percent, electrolyte and 80 percent electrolyte file, which defined the choice of the parameters of impregnation, electrolyte concentration, and fill. Fourteen identical cells were built with the parameter values described in Table 3-17.

3.3.2 Construction of Cells

Each cell consisted of four negative and three positive electrodes. Electrode characteristics are given in Table 3-18. The positive electrodes were of the same batch as used for previously built cells and were characterized in Table 3-18. The setting of interelectrode distance, and calculation of residual void value of core was performed as described previously. The number of electrodes in each cell was reduced to four negative and three positive because any greater number of positive would have resulted in a N/P ratio of less than 1.4/1 which would not have allowed a setting of 40 percent precharge.

Table 3-18. Characteristics of 1.8 g/cm^3 Void Negative Electrodes

Thickness	0.031 in.
Capacity	1.55 Ah
Residual Porosity	36.5 %

The 14 identical cells were each equipped with a pressure transducer and given a precharge of 40 percent by venting oxygen gas to an equivalency of 1.6 Ah (1.6 Ah corresponding to a venting of 45 psi of oxygen since the cell void volume was equal to 115 cc).

3.3.3 Test Cycling of Cells with Optimum Hydrogen Recombination Capability

All 14 cells were given 30 conditioning cycles at a C/4 charge (1 ampere) for 3 hours and a C/2 (2A) discharge for 1 hour. Two cells were subjected to destructive physical analysis (DPA) immediately after the completion of conditioning cycling. The other 12 cells were subjected to simulated geosynchronous orbit cycling at 75 percent depth of discharge with mid- and end-of-season reversals. At the end of each season, after end-of-season reversal, two cells were removed from cycling and subjected to destructive physical analysis (DPA) except after season four as explained below. Thus, cells were subjected to DPA, two of which had no seasons of cycling and no reversal, two had one season, two had two seasons, two had three seasons, two had five seasons, two had six seasons, and, finally, two had seven seasons of geosynchronous orbit cycling plus extensive reversal. Prior to the beginning of fourth season cells were accidentally not subjected to precharge adjustment, which was discovered after midseason reversal, therefore cells were not subjected to end-of-season reversal and no cells were removed for DPA after the fourth season.

Cells were subjected to midseason overdischarge at 1 ampere (C/4) and at 0.4 ampere (C/10) at the end of season during the first four seasons. Thereafter during Seasons 5 through 7 the midseason overdischarge rate was decreased to 0.4 ampere and the end of season to 0.2 ampere (C/20) because of decreasing hydrogen recombination rates.

Cells were overdischarged until cell voltage reached -0.5 volt.* Any cell which did not reach -0.5 volt continued to overdischarge for the time period prescribed in Table 3-19.

Cells which did reach -0.5 volt were subjected to subsequent overdischarge cycle during the season without further adjustment. Table 3-20 lists the total ampere-hours of reversal that each cell was given for each season. Immediately beneath the season number is the maximum possible ampere-hours of reversal based on times, rate, and frequency of reversal for each season. Precharge adjustments were made on cells before beginning

*Indicates exhaustion of electrochemically available precharge.

Table 3-19. Overdischarge Rates at Times for Optimum Design Cells Subjected to Cycling and Overdischarge

Season Number	Overdischarge Rates and Times					
	Cycle 22		Cycle 23		Cycle 45	
	Time	Rate	Time	Rate	Time	Rate
1	10 min	1 A	-	-	10 min	1 A
2	60 min	1 A	60 min	1 A	2 hr	0.4 A
3	60 min	1 A	60 min	1 A	2 hr	0.4 A
4	60 min	1 A	60 min	1 A	None	
5	60 min	0.4 A	60 min	0.4 A	2 hr	0.2 A
6	60 min	0.4 A	60 min	0.4 A	2 hr	0.2 A
7	60 min	0.4 A	60 min	0.4 A	2 hr	0.2 A

Table 3-20. Total Ampere-Hours of Reversal for Each Cell During Each Season (Ah)

Cell No.	Season No.						
	1	2	3	4	5	6	7
3	0.32						
9	0.18						
1	0.32	1.93					
11	0.32	2.22					
4	0.32	2.25	2.8				
14	0.21	1.21	0.61				
6	0.18	0.63	0.65	0.35	1.0		
13	0.32	2.08	1.76	0.95	1.2		
10	0.32	1.59	2.13	0.52	1.2	1.08	
12	0.32	2.28	2.8	1.8	1.2	0.9	
2	0.32	2.19	2.16	1.02	1.2	1.2	0.96
8	0.21	1.57	2.3	0.76	1.2	1.0	0.94
Maximum Allowed (Ah)	0.32	2.8	2.8	2.0	1.2	1.2	1.2

Seasons 3, 5, 6, and 7. Adjustments for cells which did not reach -0.5 volt during the last overdischarge of the previous season consisted of evacuating hydrogen from cells, overcharging cells and venting oxygen equal to half the pressure of hydrogen removed by evacuation. For cells whose voltage reached -0.5 volt during the last overdischarge of the previous season, oxygen was vented equivalent to 1.6 Ah of precharge (45 psi).

During the seven seasons of simulated geosynchronous orbit cycling with three extensive overdischarge per season, no cell shorts were experienced. No cell pressure in excess of 80 psig development and no cell reached undervoltage during geosynchronous orbit cycling indicating maintenance of cell capacity. A total of 130 extensive cell reversals were experienced. Table 3-21 lists the cell capacities to 1.0 volt during the final discharge of each season. The results in general indicate that despite extensive and repetitive reversals, cells retained their capacity.

Table 3-21. Capacities (Ah) of Optimized Cells Subjected to Geosynchronous Orbit Cycling Simulation Plus Reversal

Cell No.	Season No.					
	1	2	3	4	5	6
5	X	X	X	X	X	X
7	X	X	X	X	X	X
3	1.0	X	X	X	X	X
9	3.7	X	X	X	X	X
1	4.3	2.7	X	X	X	X
11	4.4	2.9	X	X	X	X
4	3.0	3.0	2.9	X	X	X
14	3.8	3.4	2.0	X	X	X
13	4.2	3.6	3.1	3.9	X	X
6	3.1	3.2	3.4	3.0	X	X
10	4.3	4.0	0.9	3.5	3.0	X
12	3.8	3.3	3.4	3.6	3.4	X
2	4.4	3.4	2.1	4.0	3.4	3.7
8	4.1	3.3	2.9	3.0	3.0	3.5

The average hydrogen recombination rate during reversal after midseason was calculated for each cell by the equation:

$$I_{recomb} = I_{overdis} - \frac{2FV}{RT}\frac{\Delta P}{\Delta t}$$

where $I_{overdis}$ = 1.0 or 0.4 or 0.2 ampere.

Table 3-22 lists the hydrogen recombination rates for each overdischarge performed on each cell for every season. The first two overdischarges (except for Season 1) represent midseason reversals after Cycles 22 and 23 and the third overdischarge represents reversals at the end of the season after Cycle 45.

The midseason recombination rate as measured during overdischarge after the 22nd and 23rd cycles was plotted versus eclipse season number in Figure 3-11. As the data show, the recombination rate decreases from season to season but increases from the 22nd cycle to the 23rd within each season. This sequence effect was noted and described in Section 3.1.3 involving the pressure end temperature versus recombination rate study.

After completing overdischarge at the end of each season, two cells were removed from cycling and subjected to destructive physical analysis (DPA). Table 3-23 outlines the results of DPA for cells removed from cycling. The data in Table 3-23 shows (a) a gradual removal of electrolyte from the separator, which does not necessarily correspond to positive electrode swelling (about half of the positive electrode swelling occurred during the 30-cycle burn in); (b) a considerable amount of undischargeable cadmium capacity especially since many cells had been overdischarged (during the overdischarge following the 45th cycle) to -0.5 volt; and (c) essentially unchanged amount of positive and negative electrode flooded capacity based upon measurements of sample electrodes from each cell. The results shown in Table 3-21 indicated that the cells can sustain extensive and repetitive reversal without significant capacity degradation.

Table 3-22. Hydrogen Recombination Rate in Milliamperes for Each Optimized Cell for Each Overdischarge During Each Season

Overdischarge Cell	Season No.																	
	1		2			3			4		5			6			7		
	a	b	c	c	d	c	c	d	c	d	e	e	f	e	e	f	e	e	f
9	860	300																	
3	1000	0																	
1	675	0	273	443	0														
11	640	0	295	419	153														
4	1000	800	729	743	311	766	813	317											
14	780	200	475	384	0	0	0	0											
6	975	1000	870	940	0	0	64	0	1000	450	33	250	10						
13	600	0	161	362	25	0	228	0	200	450	-								
10	800	150	488	742	348	203	555	400	1000	580	66	183	35	57	85	35			
12	790	0	365	320	80	0	333	350	220	820	233	383	67	6	17	0			
2	750	106	500	575	94	216	667	222	140	720	33	216	53	31	127	0	34	120	150
8	740	200	333	406	0	57	636	100	200	600	16	153	16	10	51	18	14	210	150

a = 22nd cycle, 10 min 1 A
b = 45th cycle, 10 min 1 A
c = 22nd and 23rd cycles, 1 hour 1 A
d = 45th cycle, 2 hours 0.4 A
e = 22nd and 23rd cycles, 1 hour 0.4 A
f = 45th cycle, 2 hours 0.2 A

ORIGINAL PAGE IS OF POOR QUALITY

ORIGINAL PAGE IS
OF POOR QUALITY

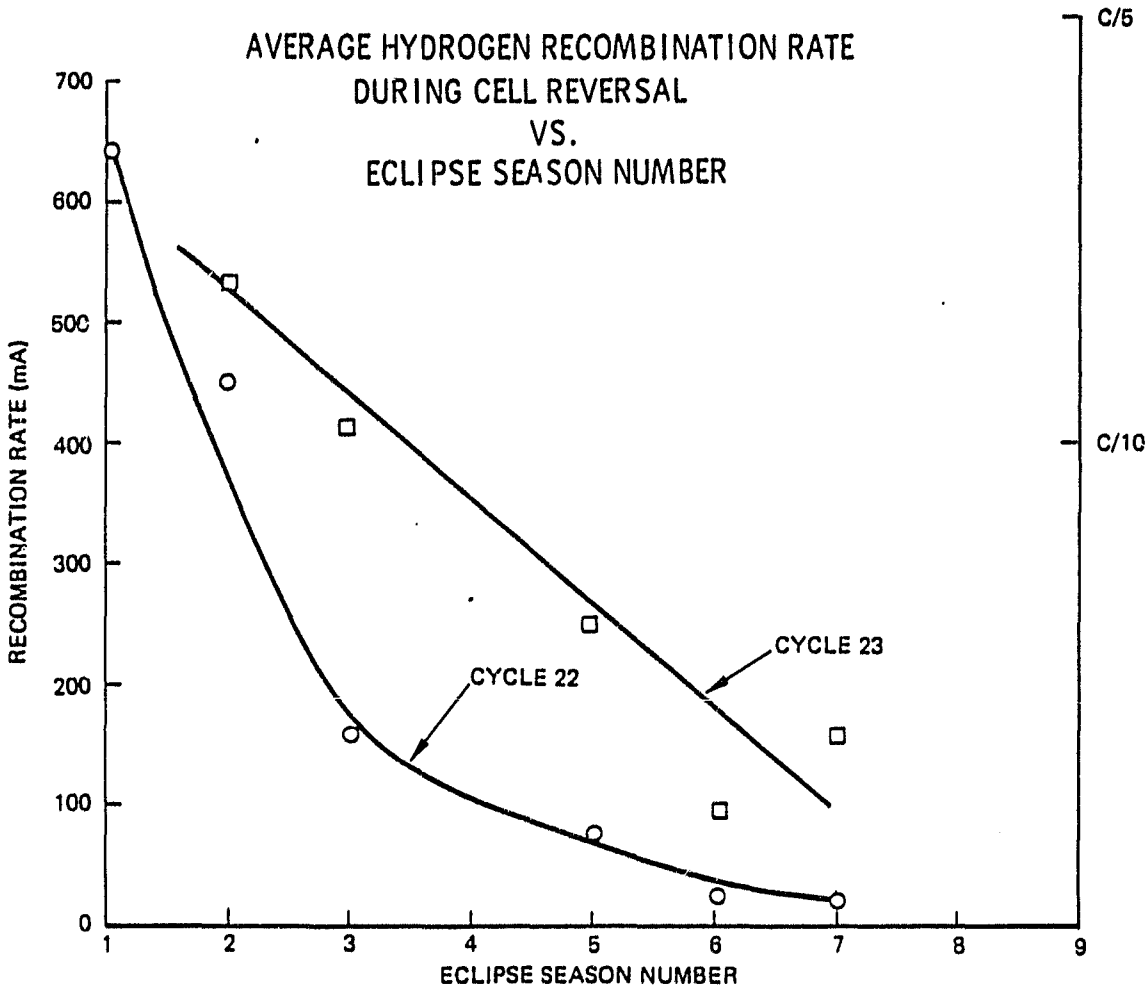

Figure 3-11. Average Hydrogen Recombination Rate During Cell Reversal Versus Eclipse Season Number

Table 3-23. Results of Destructive Physical Analyses

Cell No.	Seasons Completed Prior to DPA	Positive Electrode Thickness (mil)	Negative Electrode Thickness (mil)	Electrolyte (g/dm^2) Distribution			Flooded Capacity		Undischargeable Cadmium (Ah)
				Separator	Positive	Negative	Positive (Ah)	Negative (Ah)	
Plate	Characteristic Before Assembly of Cells	27.0	31.0	-	-	-	4.5	6.4	-
5	0	29.5	31.5	0.65	1.7	4.0	4.8	6.8	0.6
7	0	29.5	31.5	0.55	2.3	4.1	4.9	6.8	0.35
3	1	29.5	31.5	0.35	2.2	3.5	4.5	6.4	0.52
9	1	29.5	31.5	0.60	2.5	4.1	5.1	5.6	0.43
1	2	29.5	30.5	0.31	2.6	4.3	4.5	7.2	0.68
11	2	29.5	30.5	0.25	2.6	4.4	4.5	6.8	1.76
4	3	30.5	32.5	0.32	2.3	4.3	4.6	6.6	0.71
14	3	31.5	32.5	0.11	2.6	4.9	4.6	6.6	0.34
13	5*	31.5	31.5	0.39	3.0	4.3	-	8.0	0.81
6	5	31.5	31.5	0.17	2.4	4.6	5.6	7.5	1.08
10	6	32.5	32.5	0.10	2.6	4.3	4.8	6.4	0.3
12	6	31.5	32.0	0.20	2.6	4.2	4.9	6.4	0.43
2	7	32.0	32.0	0.09	2.7	4.2	5.1	6.6	0.52
8	7	32.5	32.0	0.11	2.7	4.2	4.7	6.4	0.42

*No cell removed after Season 4

3.4 EVALUATION OF LOADING LEVELS AND IMPREGNATION EFFECT ON CHARACTERISTICS OF POSITIVE AND NEGATIVE ELECTRODES FOR NICKEL-CADMIUM CELLS

The effort was now turned toward developing improved positive electrodes operated under the cell design condition which yielded optmium hydrogen recombination.

Positive electrodes of various loading and different impregnation technique were evaluated for their cyclability, specific energy, efficiency utilization and polarization characteristics.

Table 3-24 lists the different positive electrodes evaluated differing from each other with respect to active material loading and method of impregnation.

Table 3-24. Varities of Positive Electrodes for the Positive - Positive Cells

Loading Level		Impregnation Chemical	Method Electrochemical
g/dm^2	g/cm^3 void		
9.9	1.8		$\mu = 2$
8.8	1.6	$\mu = 2$	$\mu = 2$
7.7	1.4	$\mu = 2$	$\mu = 2$

g = gram $Ni(OH)_2$

μ = replication

3.4.1 Utilization

The utilization of active material as determined by ETDA titration and flooded discharge at a current density of 20 mA/cm^2 (C rate) is listed in Table 3-25 along with nominal loading, measured loading, theoretical capacity, and measured capacity. A plot of utilization versus loading level of both electrochemically impregnated positive electrode and vacuum impregnated positive electrode is shown in Figure 3-12. Note that the slope Δ loading/Δ utilization is more sensitive for chemical or vacuum impregnation than for electrochemical impregnation indicating that a greater loading by vacuum impregnation results in a smaller gain in capacity than an equivalent higher loading by electrochemical impregnation. When data for vacuum

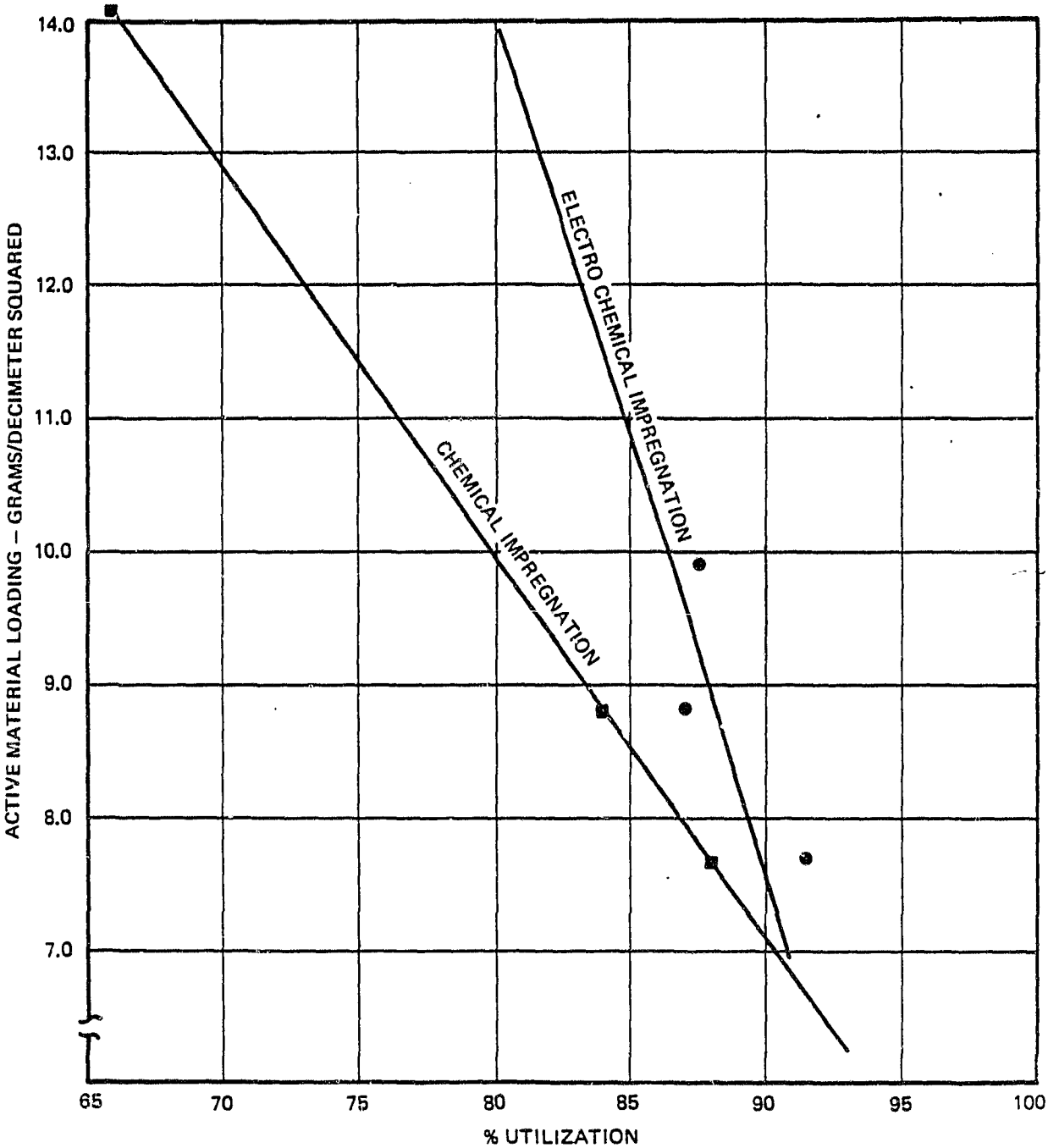

Figure 3-12. Utilization of Active Material as a Function of Impregnation Type and Loading Level

impregnation is extrapolated to 14 g/cm^2 the core parding utilization is 65 percent. General electric loads their state-of-the-art vacuum impregnated positive electrode to 14 g/dm^2 and report a utilization of approximately 65 percent.

Table 3-25. Active Material Loading as Determined by ETDA Titration, Theoretical Capacity, Measure Capacity*, and Utilization for Positive Electrodes Made by Chemical and Electrochemical Impregnation

Active Material Loading Nomigal ($gNi(OH)_2/dm^2$	Active Material Loading as Determined by ETDA Titration ($g(Ni(OH)_2/dm^2$)	Theoretical Capacity (Ah/dm^2)	Measured Capacity (Ah/dm^2)	Utilization (%)
7.7 E	7.8	2.25	2.18	96.7
7.7 Ch	7.9	2.28	2.03	89.0
8.8 E	8.9	2.57	2.35	91.4
8.8 Ch	8.9	2.57	2.25	87.5
9.9 E	10.4	3.01	2.63	87.4

D - Electrochemical impregnation

Ch - Chemical impregnation.

* - Discharge current density = 20 mA/cm^2 = C rate; electrodes where discharged under flooded condition against excess negative capacity.

3.4.2 Construction of Positive-Positive Cells

Electrode of each type were used to make two cells. Thus a total of 10 cells were constructed fcr the 5 type of electrodes. Each cell consisted of 10 electrodes of the same type with 5 electrode connected to one terminal and S other connected to the other terminal. The cell housing was the same as was shown in Figure 3-1. The interelectrode distance for each cell was set at 8 mil and electrolyte fill of residual core value was 80 percent using previously described techniques and a knowledge of electrode technician and porosity to achieve the desired design values. The electrolyte concentration was 32 percent. Thus, all of the parameter that could be set for a positive-positive cell cores pard to those in the cell design

which yielded optimum hydrogen combination. Each cell was equipped with a release valve, a pressure tranducer, and a $NiOOH/Ni(OH)_2$ reference electrode. An initial charge of one set of electrode against the metal side of the cell housing was performed. Since both sets of positive electrode in each cell were in a completely discharged state initially this method of charging avoided positive electrode reversal. Although electrode reversal would probably not be harmful, and would be experienced by the positive during over discharge in either reconditioning or in an unbalanced battery it was decided to avoid the extended reversal which would occur if one set of electrode were charged against the other set, because of possible adverse and unequal effects on the different types of electrode being compared.

Once one set of electrodes is a cell was fully charged and the other set partially completely discharged the cell could be cycled and each set of electrodes could range from 100 to 0 percent state charge with a minimum amount of overcharge of overdischarge.

3.4.3 Efficiency

With cell top temperature kept at 20°C each cell was subjected to four charge-discharge cycles at 3 ampere, C/2 so that each set of electrodes received two charges and two discharges at C/2. A discharge or charge was considered complete when discharging set of electrode exhibited a voltage of -200 mV versus the $NiOOH/Ni(OH)_2$ reference electrode. Following the completion of a discharge at 3A a supplemental discharge at 600 mA to the same cutoff voltage was performed.

After determining 100 percent cell capacity for each set of cell electrodes (listed in Table 3-26) charge inputs representing 40, 60, and 80 percent of that value were made at 3.0 ampere. Following each charge inputs cells were discharged at 3.0 ampere to a discharging electrode set to reference voltage of -200 mV. The discharge was supplemented at 600 mA to the same voltage cutoff prior to going on to the next charge input.

ORIGINAL PAGE IS
OF POOR QUALITY

Table 3-26. Measured Capacities for Positive-Positive Cells

Cell No.	Type	Capacity (Ah)
1	7.7 E	6.0
2	7.7 E	5.0
3	7.7 Ch	5.0
4	7.7 Ch	6.0
5	8.8 E	6.3
6	8.8 E	5.5
7	8.8 Ch	5.8
8	8.8 Ch	6.0
9	9.9 E	7.2
10	9.9 E	6.8

Table 3-27 lists the average efficiency at 40, 60, and 80 percent state of charge.

Table 3-27. Efficiency as a Function of Loading Levels Type of Impregnation and Stage of Charge

Impregnated Type	Loading Level		Percent Efficiency at Given State of Charge		
	g/dm^2	g/cm^3 void	40%	60%	80%
Electrochem	9.9	1.8	86	89	91
Chem	8.8	1.6	83	84	89
Electrochem	8.8	1.6	82	88	88
Chem	7.7	1.4	80	88	92
Electrochem	7.7	1.4	84	88	93

The data does not indicate any significant difference in efficiency as a function of type impregnation or active material loading. The only trend indicated is an increase in efficiency with increasing state of charge for all electrode types tested. (This is somewhat unexpected but this trend had been noted before in an internally funded TRW IR&D program on charge management of state-of-the-art nickel-cadmium cells in 1974-1975.)

3.4.4 Polarization

In order to achieve polarization value at the voltage plateau of the positive electrode all cells were brought to 50 percent state of charge. This meant that both sets of electrodes in each cell were at 50 percent state of charge and polarization data for both sets of electrode could be taken simultaneously one set for charge the other for discharge at the voltage plateau region.

All cells were subjected to sequentially ascending and discending charge and discharge currents of magnitude and duration as shown in Table 3-28 below. The positive to reference voltage was measured for both sets of electrode for both charge and discharge currents thus establishing polarization measurements in both the charge and discharge direction for both sets of electrode for each of the 10 cells and 5 electrode type. The average cell capacity was 6.0 Ah. Thus the range of perturbation from 50 percent state of charge is from +11.5 to 4 percent or from 61.5 to 46 percent SOC or DoD depending upon which electrode set is considered.

This range is well within the plateau region of the postiive electrode meaning that polarization data was taken at a region not close to completely discharged a completely charge states were voltage would be fluctuating with a small input or output of charge.

The polarization of each cell at a particular current was determined by calculating the difference of the measured postive-to-reference voltage or open circuit and the measured postive-to-reference voltage at that particular current. Figure 3-13 is a plot of the average charge and discharge polarization for the 3 levels of impregnation of positive electrodes made by electrochemical impregnation. Figure 3-14 shows similar data for the two loading levels of vacuum impregnated electrodes. Polarization data did not indicate a particular trend either with respect to loading or type of impregnation.

Table 3-28. Current, Times and Ampere-Minutes for Polarization Test

Charge			Discharge		
Current (A)	Time (Min)	Charge (Amin)	Current (A)	Time (Min)	Charge (Amin)
0.3	5	1.5	-6.0	2	12
0.6	3	1.8	-3.0	3	9
1.2	3	3.6	-1.2	3	3.6
3.0	2	6.0	-0.6	5	3.0
6.0	2	12.0	-0.3	5	1.5
3.0	2	6.0	-0.6	5	3.0
1.2	3	3.6	-1.2	3	3.6
0.6	3	1.8	-3.0	3	9.0
0.3	5	1.5	-6.0	2	12.0
Total (Amin)		40.8			-56.7
Total (Ah)		0.68			-0.93

3.4.5 Cycling Tests and Distructive Physical Analysis

After the completion of polarization testing one each of the five different design positive-positive cells was removed from tests and subjected to destructive physical analysis. The remaining five positive-positive cells were subjected to continuous cycling at C/5 (1.2A) for a period of 2.5 hours in both the charge and discharge direction. Cycling was terminated after 200 cycles to allow for DPA of the five cycled cells within the time period and budget of the contract.

The cycling based on an average cell capacity of 6 Ah was designed to maintain the depth of discharge of both sets of positive electrodes in each cell at approximately 50 percent depth of discharge, thereby minimizing overdischarge in either direction. Whenever an overdischarge manifested itself as indicated by an end of charge (or discharge) cell voltage greater than $\pm$1.0 V appropriate adjustments were made in the following cycle by reducing charge or discharge time by a few minutes and then returning to a full time period (2-5 hours) or charge and discharge or subsequent cycles.

OF POOR QUALITY

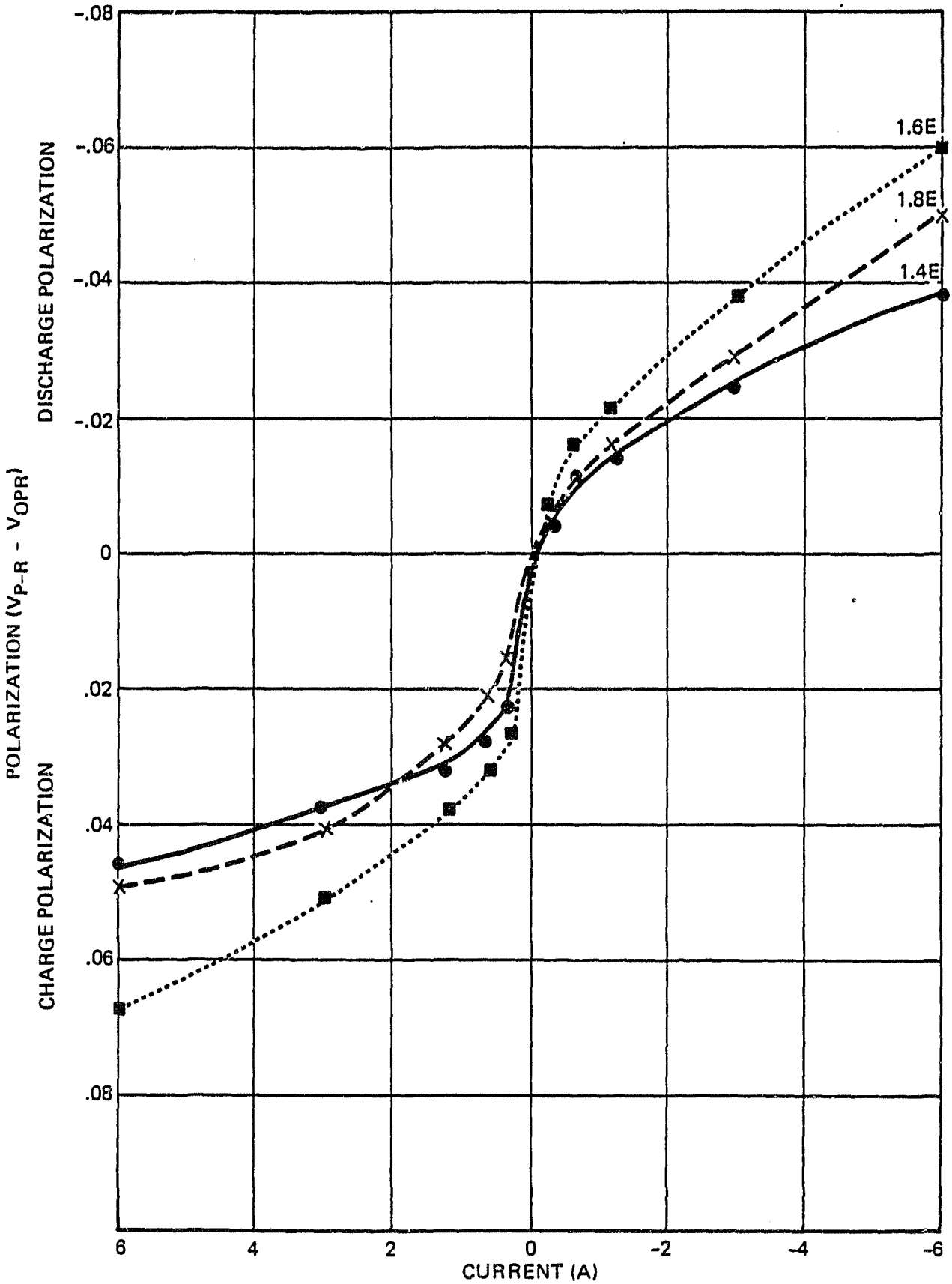

Figure 3-13. Polarization Versus Current Electrochemical Impregnation Positive Electrodes

ORIGINAL PAGE IS
OF POOR QUALITY

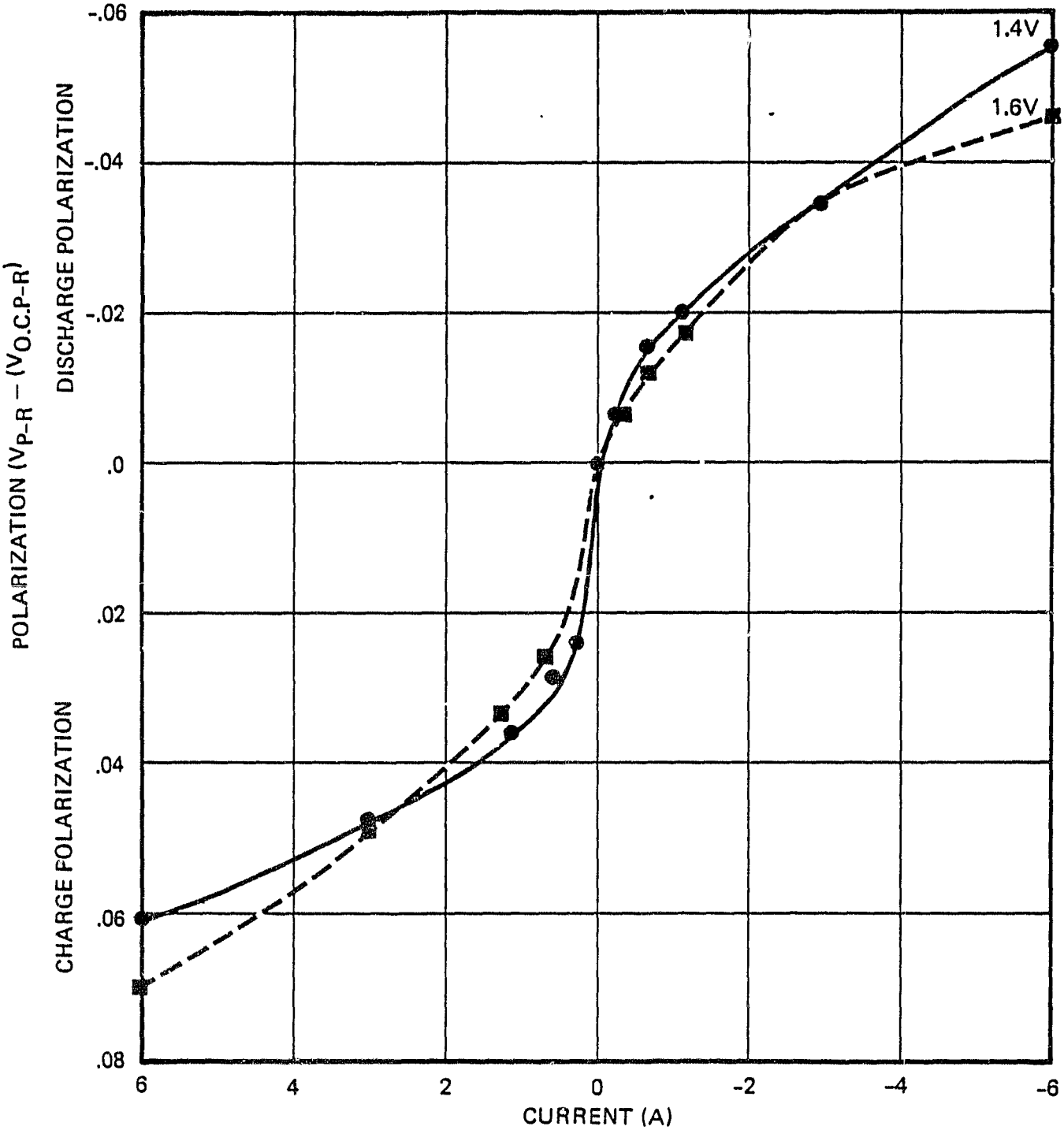

Figure 3-14. Polarization Versus Current Vacuum Impregnated Positive Electrodes

Tables 3-29 and 3-30 lists the results DPA before and after cycles for the five different positive electrode type cells. Table 3-29 shows electrode thickness and electrolyte distribution before and after cycling. While no significant electrode thickening was noted electrolyte was lost from the separator as a result of cycling for every electrode type except the 8.8 g/cm^2 electrochemically deposited which indicated an increased electrolyte content in the separator after cycling.

Table 3-30 shows electrolyte composition prior to and after cycling in the positive electrodes and separator for each cell type. Undischargeable nickel after cycling in the charged and discharged state of the different electrode is also shown. No significant difference in KOH/K_2CO_3 levels as a function of cycling or different electrode type were noted. The charged positive electrode of the 8.8 g/cm^2 chemical impregnated type exhibited a high amount of undischargeable nickel. Since this exceeded the loading level the measurement may have been in error.

Table 3-29. Electrode Thickness and Electrolyte Distribution Before and After Cycling in Positive-Positive Cells

Electrode Type	Electrode Thickness (mil)				Electrolyte Distribution (g/dm^2)					
	Prior to Cycling		After Cycling		Prior to Cycling			After Cycling		
	Charged	Discharged	Charged	Discharged	Pos (Ch)	Pos (Dis)	Sep	Pos (Ch)	Pos (Dis)	Sep.
7.7 CH	29.0	28.0	28.5	28.0	4.1	3.7	0.92	3.9	3.6	0.6
7.7 ED	27.5	27.5	27.0	27.5	3.4	3.6	1.2	3.9	3.6	0.7
8.8 CH	28.5	27.5	29.5	28.0	3.5	3.3	0.93	3.8	3.3	0.8
8.8 ED	28.0	27.5	27.5	27.5	3.9	3.1	0.85	3.7	3.3	1.1
9.9 ED	28.5	28.5	30.0	28.0	3.2	2.5	1.1	3.6	3.0	0.5

Table 3-30. Electrolyte Composition: Undischargeable Nickel in Positive-Positive Cells

Electrode Type	Electrolyte Composition KOH/K_2CO_3 (g/dm^2)					Undischargeable Nickel (g/dm^2)		
	Prior to Cycling			After Cycling			After Cycling	
	Pos (Ch)	Pos (Dis)	Separator	Pos (Ch)	Pos (Dis)	Separator	Charged	Discharged
7.7 CH	1.0/0.95	0.9/0.4	0.17/0.13	0.98/0.70	0.99/0.35	0.12/0.09	7.7	1.8
7.7 ED	0.96/0.08	0.88/0.5	0.29/0.18	1.2/0.78	0.85/0.62	0.11/0.16	8.1	2.5
8.8 CH	1.2/0.62	0.95/0.46	0.19/0.16	1.1/0.55	0.91/0.36	0.17/0.10	10.0	1.8
8.8 ED	1.0/0.97	0.92/0.37	0.14/0.18	1.1/0.77	0.95/0.59	0.23/0.21	7.8	1.7
9.9 ED	0.82/0.85	0.70/0.42	0.15/0.22	1.3/0.69	0.67/0.57	0.68/0.12	10.5	2.4

4. SUMMARY OF RESULTS

The hydrogen recombination mechanism, which has explained the behavior of nickel cadmium cells during voltage reversal has been verified and expanded. The mechanism states that hydrogen generated at the positive electrode during the reversal of a sealed nickel-cadmium cell reacts with the discharged portion of the negative electrode $Cd(OH)_2$ to form cadmium and water, $H_2 + Cd(OH)_2 \rightarrow 2H_2O + Cd$. When the rate of hydrogen generation as measured by the overdischarge current and its consumption as measured by the recombination current are equal the cell may be overdischarged indefinitely without change in pressure or exhaustion of negative capacity. It was also shown that the rate of hydrogen recombination during voltage reversal is directly proportional to the hydrogen pressure, and almost independent of temperature.

State-of-the-art cells exhibit recombination or overdischarge rates as high as C/100. This finding suggest that with optimization of certain critical cell parameters it would be possible to increase hydrogen recombiantion rate and hence safe overdischarge rate significantly. By the development of battery cells with increased overdischarge capability greater flexibility in reconditioning rate selection would be possible as well as reduction of the complexity of battery bypass circuity. A battery made with such cells and without bypass circuity result in lower cost, lower weight and higher reliability, thereby permitting growth in payload size and spacecraft life.

A parametric test was performed involving 18 different cell designs by varying impregnation method of the negative electrode, electrolyte fill of residual core void volume, electrolyte concentration, interelectrode distance loading level of the negative electrode and precharge.

The parametric testing lead to the development of a laboratory cell capable of sustaining a C/2 overdischarge rate without developing excessive pressures. Fourteen cells of this optimum cell design were constructed and subjected to geosynchronous orbit cycling at 75 percent DoD with two midseason overdischarges at C/4 and an end-of-season overdischarge at C/10 for four seasons. After the fifth season rates were lowered to C/10 and

C/20 respectively. Except for the first season each midseason overdischarge was 1 hour in duration and each end-of-season overdischarge was 2 hours in duration.

During seven seasons of simulated geosynchronous orbit cycling with up to three extensive overdischarge per season no cell shorts were encountered. No cell pressure exceeded 80 psig and no cell reached under voltage during the geosynchronous orbit cycling. Capacity measurement of the cells at the end of each season indicated no significant capacity degradation.

The results of the cycling test with periodic overdischarge also demonstrated that hydrogen recombination as great as C/10 could be sustained during geosynchronous orbit cycling with cells of a particular design and that such cells could be overdischarged at rates ranging from C/4 to C/20 without detrimental effects.

Destructive physical analysis of cells removed sequentially at the rate of two after each season, did not indicate any changes that would not be encounted as a result of ordinary geosynchronous cycling without any reversal.

Positive electrodes differing in loading level and method of impregnation were tested as positive-positive cells whose design parameters where possible were the same as the cell designs which gave C/2 hydrogen recombination rates. Evalution of utilization, efficiency, polarization and cyclability were made. Results indicated that electrochemically impregnated positive electrodes have better utilization of active material than vacuum impregnated electrodes of similar loading. No difference in efficiency, polarization and cycleability was found with respect to loading level or method of impregnation.

5. CONCLUSIONS

5.1

Hydrogen recombination has been demonstrated and verified to be the mechanism which allows state-of-the-art nickel-cadmium cells to be overdischarged at low rates without excessive pressure buildup.

5.2

By optimizing critical design parameters in nickel-cadmium cells, the hydrogen recombination rate can be significantly increased over that obtainable with state-of-the-art nickel-cadmium cells.

5.3

Hydrogen recalibration rates sufficient to balance an overdischarge rate of C/10 can be sustained during geosynchronous orbit (with periodic reversal) with nickel-cadmium cells of optimized design parameters with respect to hydrogen recombination.

5.4

Optimized nickel-cadmium cells can be overdischarged at rates varying from C/10 to C/4 without detrimental effects to life and specific energy as a result of treatment or design.

5.5

A comparison of electrochemically and vacuum impregnated positive electrodes at various low levels of impregnation indicated that utilization is the only advantage gained by electrochemical impregnation. Other characteristics such as efficiency and polarization were independent of type of impregnation.

REFERENCES

1. Ritterman, P. F. Hydrogen Recombination in Sealed Nickel-Cadmium Cells, 27th Power Sources Symposium, June 1976.

2. Ritterman, P. F. The Characteristics of Sealed Nickel-Cadmium Cells During Voltage Reversal, Goddard Space Flight Center Battery Workshop, 1977.

3. Ritterman, P. F. Hydrogen Recombination in Sealed Nicke-Cadmium Aerospace Cells, 14th Intersociety Energy Conversion Engineering Conference, 1979.

4. Ritterman, P. F. Additional Reversal Characteristics of Sealed Nickel-Cadmium Cells, Goddard Space Flight Center Battery Workshop, 1979.

5. Badcock, C. Reversal of Nickel-Cadmium Cells, Goddard Space Flight Center Battery Workshop, 1979.